Geochemistry Geophysics Geosystems G3

Article
Volume 11
7 December 2010
Q0AA12, doi:10.1029/2010GC003203
ISSN: 1525-2027

Published by AGU and the Geochemical Society

Reconciling astrochronological and $^{40}Ar/^{39}Ar$ ages for the Matuyama-Brunhes boundary and late Matuyama Chron

J. E. T. Channell
Department of Geological Sciences, University of Florida, Gainesville, Florida 32611, USA (jetc@ufl.edu)

D. A. Hodell
Department of Earth Sciences, University of Cambridge, Cambridge CB2 3EQ, UK

B. S. Singer
Department of Geoscience, University of Wisconsin–Madison, Madison, Wisconsin 53706, USA

C. Xuan
Department of Geological Sciences, University of Florida, Gainesville, Florida 32611, USA

[1] When five Matuyama-Brunhes (M-B) boundary records from the North Atlantic are placed on isotope age models, produced by correlation of the $\delta^{18}O$ record directly or indirectly to an ice volume model, the M-B boundary lies consistently at the young end of marine isotope stage 19 with a mean age for the mid-point of the reversal of 773.1 ka (standard deviation = 0.4 kyr), ~7 kyr younger than the presently accepted astrochronological age for this polarity reversal (780–781 ka). Two recently proposed revisions of the age of the $^{40}Ar/^{39}Ar$ Fish Canyon sanidine (FCs) standard to 28.201 ± 0.046 Ma and 28.305 ± 0.036 Ma would adjust $^{40}Ar/^{39}Ar$ ages applicable to the M-B boundary (and other reversals and excursions back to 1.2 Ma) to ages older than the new astrochronological ages by 8–24 kyr. The variables used to construct the ice volume models cannot account for the discrepancy. The FCs standard age that best fits the astrochronological ages is 27.93 Ma, which is within the uncertainty associated with the commonly used value of 28.02 (±0.16) Ma but younger than the recently proposed FCs ages. The EDC2 and EDC3 age models in the Dome C (Antarctic) ice core yield ages of 771.7 ka and 766.4 ka, respectively, for the ^{10}Be flux peak that denotes the paleointensity minimum at the reversal boundary, implying that the EDC2 (rather than EDC3) age model is consistent with the observations from marine sediments, at least close to the M-B boundary.

Components: 10,700 words, 13 figures, 2 tables.

Keywords: argon ages; magnetic reversals; astrochronology; magnetic excursions; Matuyama-Brunhes boundary.

Index Terms: 1535 Geomagnetism and Paleomagnetism: Reversals: process, timescale, magnetostratigraphy; 1115 Geochronology: Radioisotope geochronology; 4910 Paleoceanography: Astronomical forcing.

Received 3 May 2010; **Revised** 21 September 2010; **Accepted** 23 September 2010; **Published** 7 December 2010.

Channell, J. E. T., D. A. Hodell, B. S. Singer, and C. Xuan (2010), Reconciling astrochronological and $^{40}Ar/^{39}Ar$ ages for the Matuyama-Brunhes boundary and late Matuyama Chron, *Geochem. Geophys. Geosyst.*, *11*, Q0AA12, doi:10.1029/2010GC003203.

Theme: EarthTime: Advances in Geochronological Technique
Guest Editors: D. Condon, G. Gehrels, M. Heizler, and F. Hilgen

1. Introduction

[2] The Matuyama-Brunhes (M-B) boundary often constitutes a “golden spike” in the age calibration of sediment sequences. Knowing the age of this polarity chron (reversal) boundary is therefore important to a wide range of studies, although the duration, and possibly the age, of this and other polarity reversals is likely to be a function of site location at scales of a few millennia [*Clement*, 2004; *Leonhardt and Fabian*, 2007]. The currently popular age for the M-B polarity chron boundary (780 ka) comes from *Shackleton et al.* [1990], although the reversal age was adjusted to 781 ka in a more recent time scale [*Lourens et al.*, 2004]. The publication of *Shackleton et al.* [1990] was revolutionary because it placed the polarity chron boundary 50 kyr older than the previously accepted age (730 ka) based on astrochronologies in marine sediments [*Imbrie et al.*, 1984; *Ruddiman et al.*, 1989] and K-Ar radioisotopic ages [see *Mankinen and Dalrymple*, 1979]. The new age implied a systematic (~7%) error in K-Ar ages over the last few Myr, and that previous astrochronologies for the Brunhes chron had “lost” an obliquity cycle (or two precessional cycles). A similar astrochronological age for the M-B boundary (790 ka) was suggested some 8 years earlier [*Johnson*, 1982], however, it took the better constrained estimate of *Shackleton et al.* [1990] to achieve the necessary traction to overturn the younger (730 ka) age.

[3] The 780 ka age for the M-B boundary was based on astronomical tuning of benthic and planktic $\delta^{18}O$ records from Ocean Drilling Program (ODP) Site 677 in the eastern equatorial Pacific [*Shackleton et al.*, 1990]. The isotope records from ODP Site 677 were matched to an ice volume model [*Imbrie and Imbrie*, 1980] that was based on the orbital (insolation) solutions of *Berger and Loutre* [1988]. The procedure was aided by a strongly modulated precession signal in the planktic isotope record (the modulation helping to check for “lost” precession cycles) and a strong obliquity signal in the benthic record. Unfortunately, magnetic stratigraphy could not be obtained at Site 677, and therefore the position of the M-B boundary at Site 677 was unknown. To place the M-B boundary in the Site 677 age model, *Shackleton et al.* [1990] transferred the M-B boundary from Deep Sea Drilling Project (DSDP) Site 607 to ODP Site 677 by correlation of the two isotope records (Figure 1). The position of the M-B boundary at Hole 607A is known within a few centimeters at 31.84 m depth [*Ruddiman et al.*, 1989] and this level was transferred to the 30.40 m level at Site 677, indicating very similar mean sedimentation rates for the Brunhes Chron at the two sites (~4 cm/kyr).

[4] In the last few years, several high sedimentation rate records, with mean sedimentation rates in the 7–17 cm/kyr range, have become available which provide higher-resolution isotope-paleomagnetic correlations across the M-B boundary. In addition, the European Project for Ice Coring in Antarctica (EPICA) has now obtained deuterium measurements (δD_{ice}) at Dome C to 3260 m depth, beyond the M-B boundary [see *Jouzel et al.*, 2007]. The current time scale at Dome C (EDC3) [*Dreyfus et al.*, 2007; *Parrenin et al.*, 2007] has evolved from that provided earlier (EDC2) by *EPICA Community Members* [2004]. EDC3 is based on an accumulation and ice flow model (as for EDC2), however, it is constrained by orbital tuning of air content and $\delta^{18}O_{air}$ records. The position of the M-B boundary can be estimated from ^{10}Be flux measurements at Dome C [*Raisbeck et al.*, 2006; *Dreyfus et al.*, 2008].

[5] Advances in $^{40}Ar/^{39}Ar$ geochronology including incremental heating of groundmass separates, spurred by the *Shackleton et al.* [1990] astronomical ages for the last several polarity reversals, led to the first direct dating of lava flows thought to record the M-B reversal [*Baksi et al.*, 1992; *Singer and Pringle*, 1996]. Lavas recording reverse-transitional-normal magnetization directions in flow sequences on four volcanoes have been dated using the $^{40}Ar/^{39}Ar$ method. Using the widely adopted age of 28.02 ± 0.16 Ma for the Fish Canyon sanidine (hereafter referred to as $FCs_{28.02}$) standard [*Renne et al.*, 1998], these ages range from 798.4 to 775.6 ka [*Singer et al.*, 2002; *Brown et al.*, 2004; *Coe et al.*, 2004; *Singer et al.*, 2005]. According to *Singer et al.* [2005], only the lavas on Maui record the actual M-B reversal at 775.6 ± 1.9 ka, which was apparently preceded by a period of transitional and weakened field, as recorded by the other lava flows between about 798 and 792 ka. Although a paleointensity low does appear in sedimentary records at ~792 ka, transitional magnetization directions of this age have not been recorded in sediments.

[6] Recently *Kuiper et al.* [2008] proposed a calibration of the FCs standard that shifts its age to 28.201 ± 0.046 Ma, based on $^{40}Ar/^{39}Ar$ dating of tephra deposits in the Miocene Melilla basin for which astrochronologic age control is available. Subsequently, *Renne et al.* [2010] proposed an FCs standard age of 28.305 ± 0.036 Ma based on a statistical optimization that includes pairs of ^{238}U-^{206}Pb and $^{40}Ar/^{39}Ar$ data from selected samples. It is important to note that the *Kuiper et al.* [2008] and

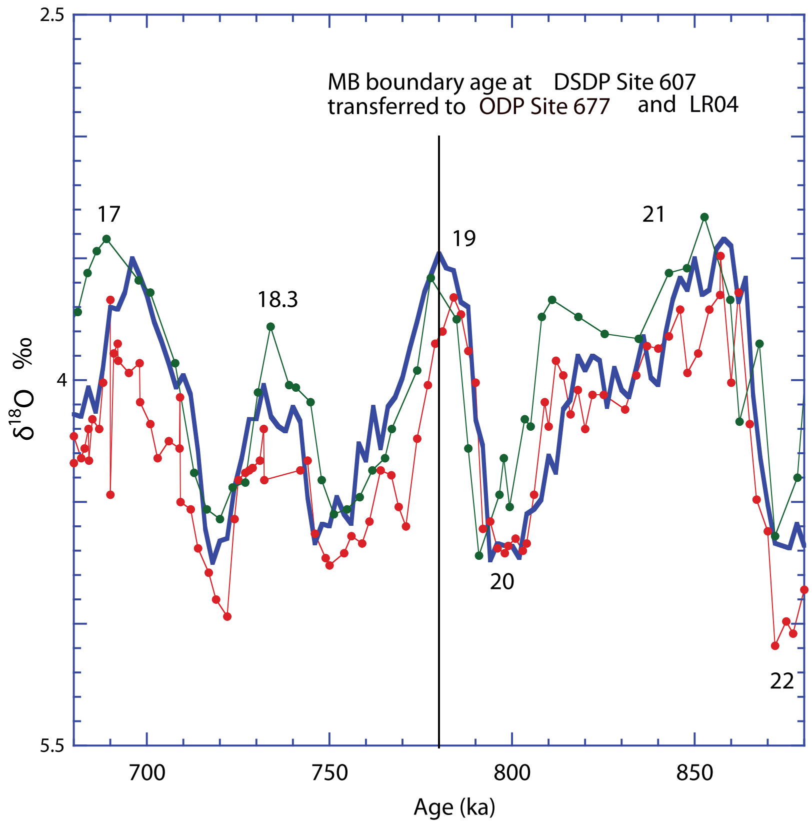

Figure 1. Benthic oxygen isotope data from DSDP Site 607 (green [*Ruddiman et al.*, 1989]), ODP Site 677 (red [*Shackleton et al.*, 1990]), and the LR04 benthic oxygen isotope stack (blue [*Lisiecki and Raymo*, 2005]) placed on their independent age models. Marine isotope stages are numbered, and the traditional age (780 ka) of the Matuyama-Brunhes (M-B) boundary is indicated.

Renne et al. [2010] ages for FCs use total ^{40}K decay constants of 5.463×10^{-10} a^{-1} and 5.5492×10^{-10} a^{-1}, respectively, that differ from the value of 5.543×10^{-10} a^{-1} recommended by *Steiger and Jaeger* [1977]. If adopted, these recently proposed FCs standard ages, hereafter denoted FCs$_{28.201}$ and FCs$_{28.305}$, would shift the age of the lava flows on Maui, and hence the ^{40}Ar/^{39}Ar age of the M-B reversal, to 781 ka and 784 ka, respectively, both of which conflict with the astrochronologic estimates discussed here.

2. North Atlantic Sediment Cores

[7] Coupled isotope-paleomagnetic records across the M-B boundary are available for numerous marine cores (see review by *Tauxe et al.* [1996]) although very few have sedimentation rates exceeding a few cm/kyr, and fewer still have coupled isotope-paleomagnetic records at high resolution across the boundary interval. Five sites that satisfy the criteria of high (>5 cm/kyr) sedimentation rates and high-resolution coupled isotope-paleomagnetic records are North Atlantic ODP Sites 980, 983, 984, 1063 and Integrated Ocean Drilling Program (IODP) Site U1308 (Figure 2).

[8] We compare the position of the M-B boundary relative to δ^{18}O data at these five sites, to provide estimates for the age of the M-B boundary. The directional magnetic data across the M-B boundary can be represented as virtual geomagnetic polar (VGP) latitudes, derived from magnetization components determined in a particular demagnetization interval. Normalized remanence data provide paleointensity proxies. Benthic and planktic δ^{18}O data are available over the M-B boundary interval for ODP Sites 983 and 984. Benthic δ^{18}O data (only) are available at ODP Sites 980 and 1063 and IODP Site U1308. Details concerning the determination of magnetization components and paleointensity proxies, and the oxygen isotope analyses, over the M-B boundary interval are given by *Channell and Kleiven* [2000] for ODP Site 983, *Channell et al.* [2004] for ODP Site 984, *Channell and Raymo* [2003] and *Raymo et al.* [2004] for ODP Site 980, and *Channell et al.* [2008] and *Hodell et al.* [2008]

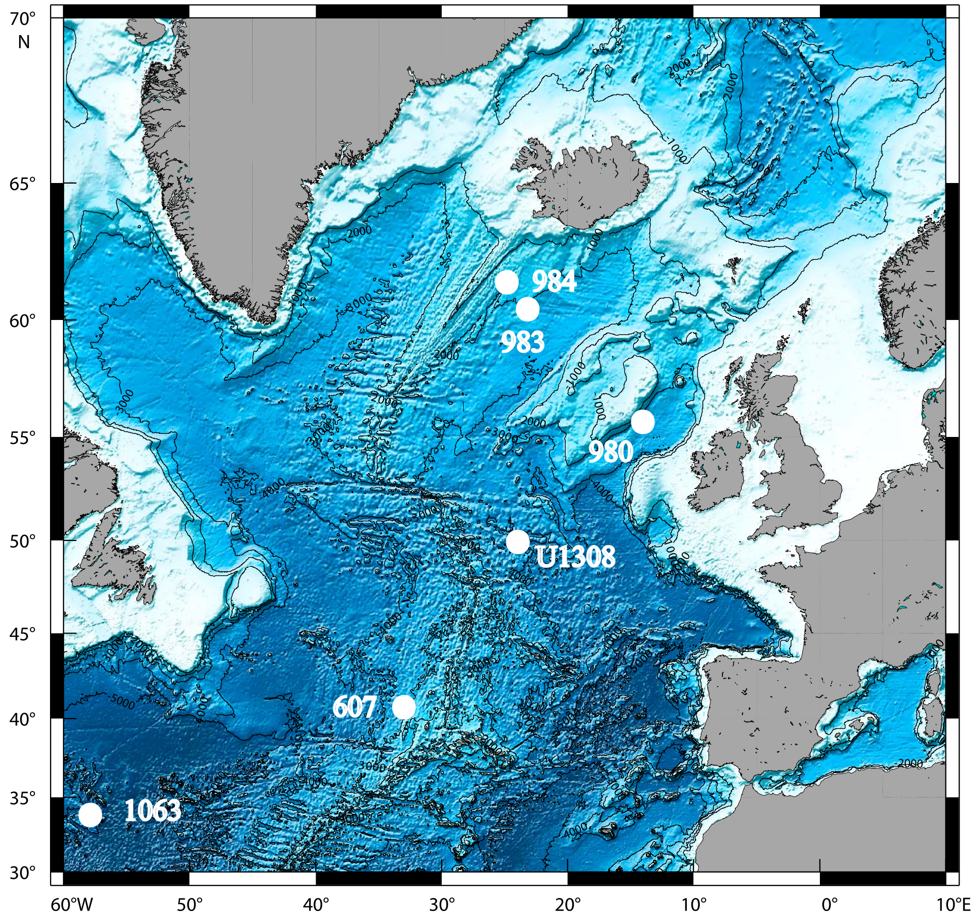

Figure 2. Map showing location of DSDP, ODP, and IODP drill sites mentioned in the text.

for IODP Site U1308. For ODP Site 1063, new magnetic and benthic oxygen isotope data were acquired across the M-B boundary to augment the oxygen isotope data of *Feretti et al.* [2005] and the magnetic data of *Shipboard Scientific Party* [1998].

[9] In Figures 3 and 4, we compare the oxygen isotope and magnetic records across the M-B boundary at ODP Sites 983 and 984. These records are compared with two alternative ice volume models [*Imbrie and Imbrie*, 1980]. One model is forced by midsummer insolation at 65°N (the traditional forcing function) based on the *Laskar et al.* [2004] orbital solution, and the other by integrated summer insolation at 65°N [see *Huybers*, 2006]. Correlation of isotope records to an *Imbrie and Imbrie* [1980] ice volume model is a widely used means of establishing the age of isotope records [e.g., *Shackleton et al.*, 1990; *Lisiecki and Raymo*, 2005]. In Figures 5 and 6, we compare the oxygen isotope and magnetic records across the M-B boundary at ODP Site 980 and IODP Site U1308. Note that age models represented in Figures 3–6 have not been adjusted for this paper, are independent of one another, and correspond to the age models given in the original publications cited above.

[10] For some of the oxygen isotope records, the resolution of the data is sufficient to extract the precessional component from the ice volume models and from the δ^{18}O records using a Gaussian bandpass filter centered on a frequency of 0.05 kyr^{-1} (period of 20 kyr) with a bandwidth of 0.02 kyr^{-1} (Figure 7). For Site U1308, the data gap in δ^{18}O caused by a barren interval just prior to the M-B boundary (Figure 6) perturbs the output; however, for Sites 983 and 984 the results support the age models.

[11] In Figure 8, we compare the Site 1063 benthic oxygen isotope record of *Feretti et al.* [2005] based on a variety of species but principally *Cibicidides wuellerstorfi* or *Nuttallides umbonifera* with oxygen isotope data from *Cibicidides wuellerstorfi* and *Oridorsalis umbonatus* measured at the University of Florida on specimens taken from u channel samples. After completion of magnetic measurements, the u channel samples with 2 × 2 cm^2 cross section

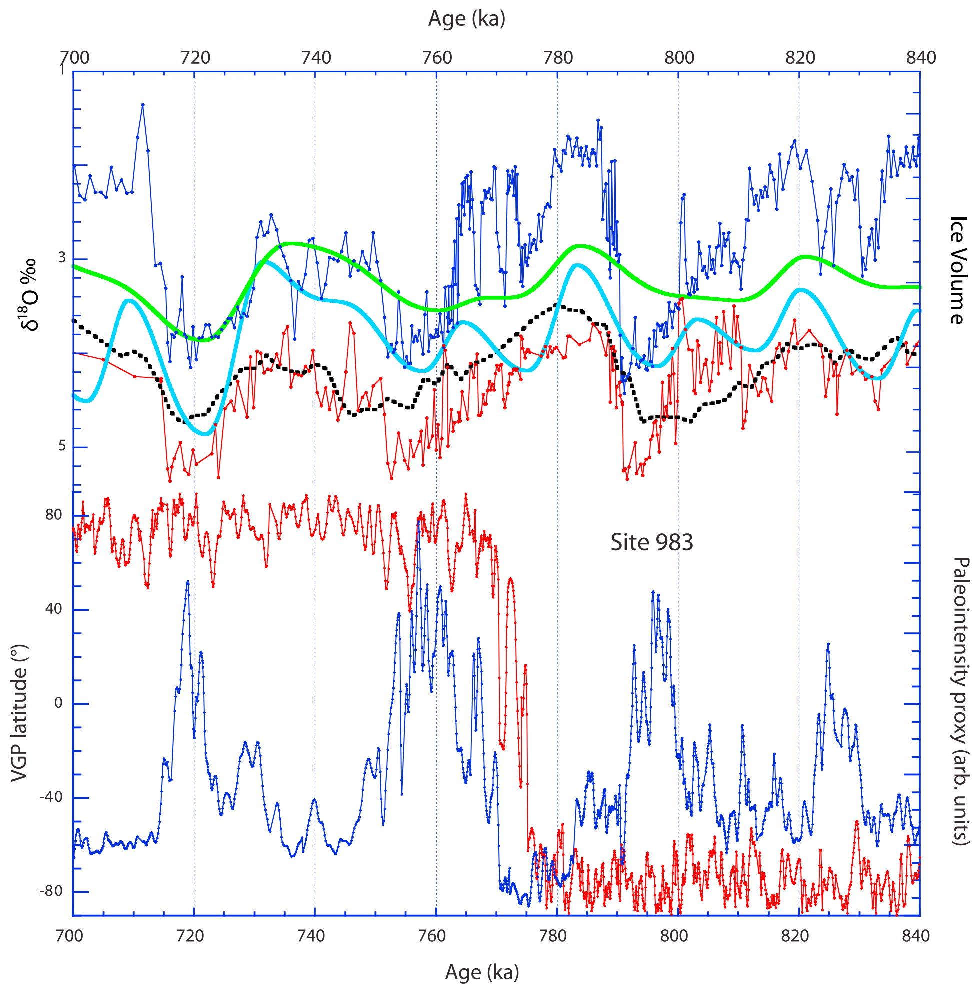

Figure 3. (top) ODP Site 983 planktic (blue) and benthic (red) oxygen isotope data compared with ice volume models based on midsummer (light blue) and integrated summer (light green) insolation forcing and LR04 from *Lisiecki and Raymo* [2005] (dashed black line). (bottom) ODP Site 983 virtual geomagnetic polar (VGP) latitude (red) and relative paleointensity proxy (blue). ODP Site 983 data from *Channell and Kleiven* [2000].

were subsampled in 5 cm intervals. Specimens were picked from the >212 μm size fraction, and one to five individuals were used for δ^{18}O analysis. The benthic δ^{18}O data of *Feretti et al.* [2005] were derived from Holes 1063A, 1063B and 1063C in the M-B boundary interval, whereas the u channel samples were taken from Hole 1063D. The δ^{18}O data of *Feretti et al.* [2005] was augmented using the u channel samples to test the shipboard hole-to-hole correlations built into the composite depth (mcd) scale. With Site 1063 data placed on a uniform age model, the alignments shown in Figure 8 indicate that the composite depth scale is consistent among holes in the M-B interval at Site 1063. Corrections for equilibrium of +0.64‰ and +0.2‰ were used for *Cibicidides wuellerstorfi* and *Oridorsalis umbonatus*, respectively.

[12] The natural remanent magnetization (NRM) components from Core 1063D-16H u channel samples were determined in the 20–80 mT peak alternating field (AF) demagnetization interval, and also by picking components individually from orthogonal projections of AF demagnetization data at 1 cm intervals (Figure 8c). Component declinations were uniformly rotated for the entire core to yield N/S declinations above/below the M-B boundary, respectively. Virtual geomagnetic polar (VGP) latitudes were calculated from the component declination and inclination data, and plotted with the maximum angular deviation (MAD) values [*Kirschvink*, 1980] associated with the NRM component directions (Figure 8c). Relative paleointensity (RPI) proxies for Site 1063 were determined from the slopes of the best fit lines of NRM versus isothermal remanence

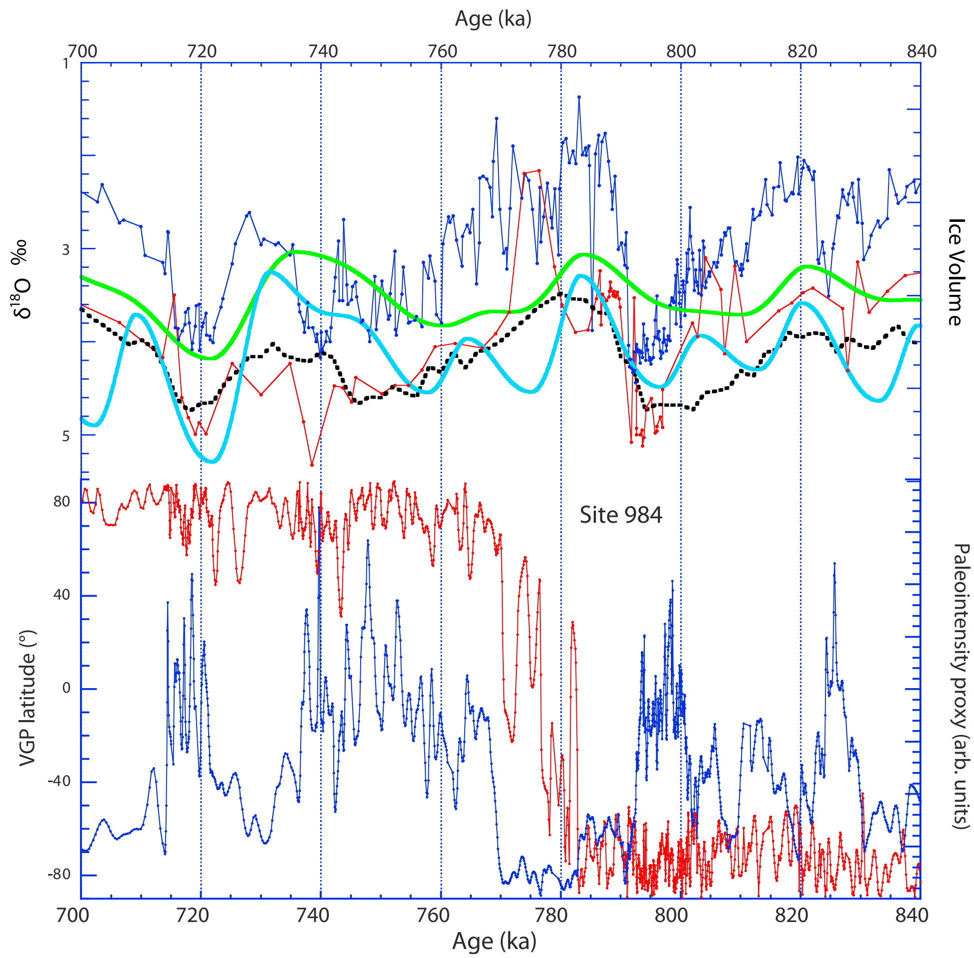

Figure 4. (top) ODP Site 984 planktic (blue) and benthic (red) oxygen isotope data compared with ice volume models based on midsummer (light blue) and integrated summer (light green) insolation forcing and LR04 from *Lisiecki and Raymo* [2005] (dashed black line). (bottom) ODP Site 984 virtual geomagnetic polar (VGP) latitude (red) and relative paleointensity proxy (blue). ODP Site 984 data from *Channell et al.* [2004].

(IRM) and anhysteretic remanence (ARM) in the 20–60 mT peak field demagnetization interval (method of *Channell et al.* [2002]). The VGP latitudes and RPI data from Site 1063 are compared with the VGP latitudes and RPI data from ODP Site 983 (Figure 8b). Note that the ODP Site 983 data are plotted on their published age model [*Channell and Kleiven*, 2000], and the Site 1063 data are plotted on an isotopic age model that appears consistent with ODP Site 983 (Figure 8a).

3. Age and Duration of the M-B Boundary in Marine Sediments

[13] Polarity reversal is a process in which the ~180° directional change in the geomagnetic field vector may take a few thousand years and the duration of the directional change depends on site location, with increasing duration at higher latitudes [*Clement*, 2004]. Modeling of the M-B boundary has been interpreted to imply a likely millennial-scale M-B boundary age discrepancy between the Atlantic and Pacific site locations [*Leonhardt and Fabian*, 2007], however, a wider distribution of high-resolution M-B boundary records, beyond the Central and North Atlantic, is needed to substantiate this finding. The estimated duration of the M-B directional transition (the time for which the VGP latitudes are below the range associated with "normal" secular variation) is quite variable: 3.5 kyr (Site 980), 4.6 kyr (Site 983), 6.2 kyr (Site 984), 4.6 kyr (Site 1063) and 2.9 kyr (Site U1308) (Table 1). This variability can be attributed to sedimentation rate changes that are not fully accommodated by the age models, and/or differences in magnetic recording efficiency and timing (lock-in) of remanence acquisition.

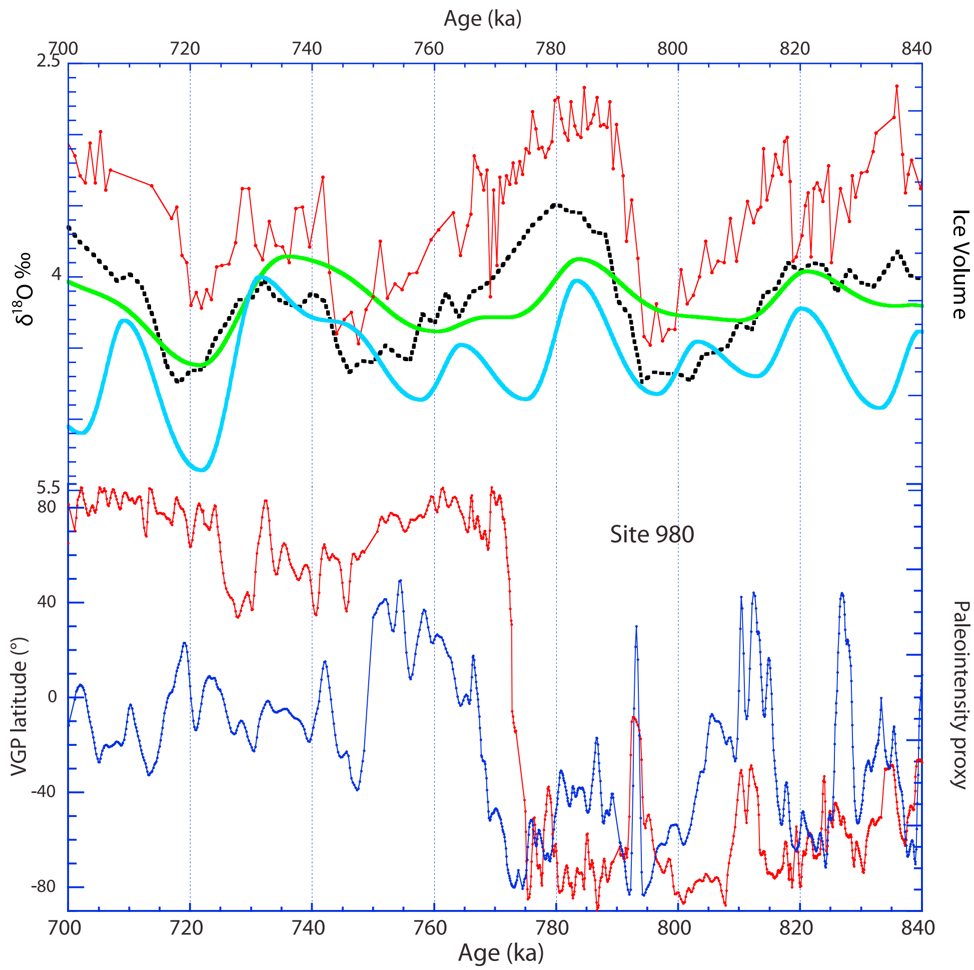

Figure 5. (top) ODP Site 980 benthic (red) oxygen isotope data compared with ice volume models based on mid-summer (light blue) and integrated summer (light green) insolation forcing and LR04 from *Lisiecki and Raymo* [2005] (dashed black line). (bottom) ODP Site 980 virtual geomagnetic polar (VGP) latitude (red) and relative paleointensity proxy (blue). ODP Site 980 data from *Channell and Raymo* [2003].

[14] The directional records across the M-B boundary at ODP Sites 983 and 984 are among the highest-resolution sedimentary records of a polarity reversal. The directional records from both sites show characteristic VGP clusters in the South Atlantic and NE Asia [*Channell and Lehman*, 1997; *Channell et al.*, 2004]. The ODP Site 984 record shows a prereversal directional "excursion" at ~781 ka that is not present at other site(s) (Figure 4). The correlation of paleointensity records between ODP Site 983 and 984, using independent age models at the two sites, supports the contention that this apparent prereversal excursion predates the onset of the reversal not only at Site 984, but also at ODP Site 983.

[15] At all five sites (Figures 3–6 and 8), the M-B directional change, as indicated by VGP latitude, occurs in the transition from marine isotope stage (MIS) 19 to MIS 18. The onset of the polarity transition certainly postdates the $\delta^{18}O$ minimum that represents the zenith of MIS 19 (MIS 19.3). Although the published age models for the five sites yield a range of duration estimates for the M-B polarity transition, the age of the midpoint of the polarity transition (labeled "reversal age" in Table 1) has a mean value of 773.1 ka and a standard deviation of 0.4 kyr.

[16] For the majority of marine cores that have yielded records across the M-B boundary, the younger age promoted here (773 ka) is more compatible with the data than the more traditional age (780 ka). Two of the higher-resolution coupled isotope-paleomagnetic records are those from Core MD900963 from the Maldives, Indian Ocean [*Bassinot et al.*, 1994] and from the ODP Site 769 from the Sulu Sea [*Oda et al.*, 2000]. For Core

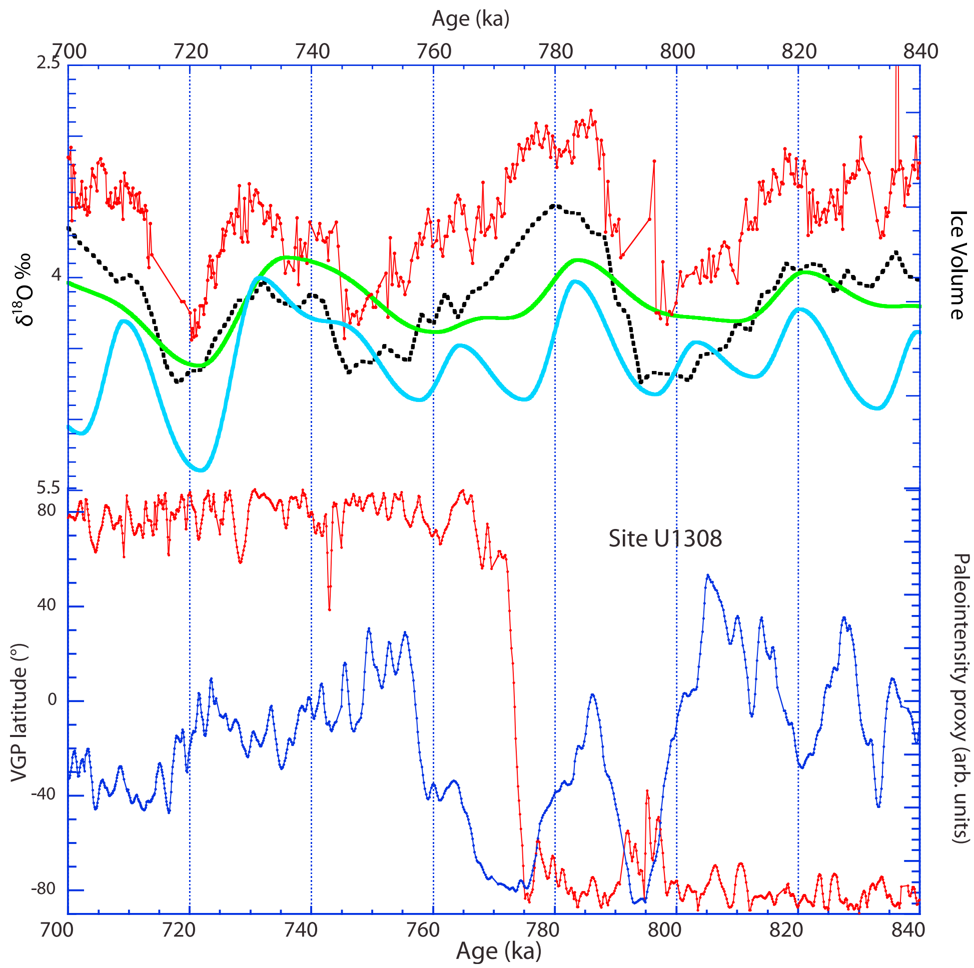

Figure 6. (top) IODP Site U1308 benthic (red) oxygen isotope data compared with ice volume models based on midsummer (light blue) and integrated summer (light green) insolation forcing and LR04 from *Lisiecki and Raymo* [2005] (dashed black line). (bottom) IODP Site U1308 virtual geomagnetic polar (VGP) latitude (red) and relative paleointensity proxy (blue). IODP Site U1308 data from *Channell et al.* [2008] and *Hodell et al.* [2008].

MD900963, the mean Brunhes sedimentation rate is 4 cm/kyr. At this site, the M-B boundary appears to lie in the MIS 19/MIS 18 transition. The planktic δ^{18}O record was correlated to an ice volume model to yield a M-B boundary age of 775 ± 10 ka [*Bassinot et al.*, 1994]. At ODP Site 769, the mean Brunhes sedimentation rate is 8 cm/kyr. The relatively high sedimentation rate is offset by the low resolution of the δ^{18}O record (one sample/20 cm). The age of the M-B boundary was determined by correlation of the planktic δ^{18}O to that of Core MD900963 yielding an M-B boundary age of 778.9 ka [*Oda et al.*, 2000]. Reestimation of the M-B boundary age at these two sites [*Tauxe et al.*, 1996], by correlation of the δ^{18}O records to an ice volume model, yielded M-B boundary ages of 776.7 ka (Core MD900963) and 776.8 ka (ODP Site 769). These age estimates exceed the M-B boundary ages estimated here (Table 1). Note, however, here that the oxygen isotope data in Core MD900963 [*Bassinot et al.*, 1994] and at ODP Site 769 [*Linsley and von Breymann*, 1991] are compromised by low sedimentation rates (Core MD900963) and low δ^{18}O sampling frequency (ODP Site 769).

4. EPICA Dome C

[17] The deep-sea benthic δ^{18}O stack (LR04 [*Lisiecki and Raymo*, 2005]) and the δD_{ice}, at Dome C [*Jouzel et al.*, 2007] are in general, although not precise, agreement back to ~800 ka (Figure 9). As the age models for the marine and ice core records are independent, this indicates a close linkage between global ice volume and Antarctic air temperatures. The close consistency of the δD_{ice} record with the CO_2 record [*Lüthi et al.*, 2008] shows that carbon dioxide concentration is also strongly correlated

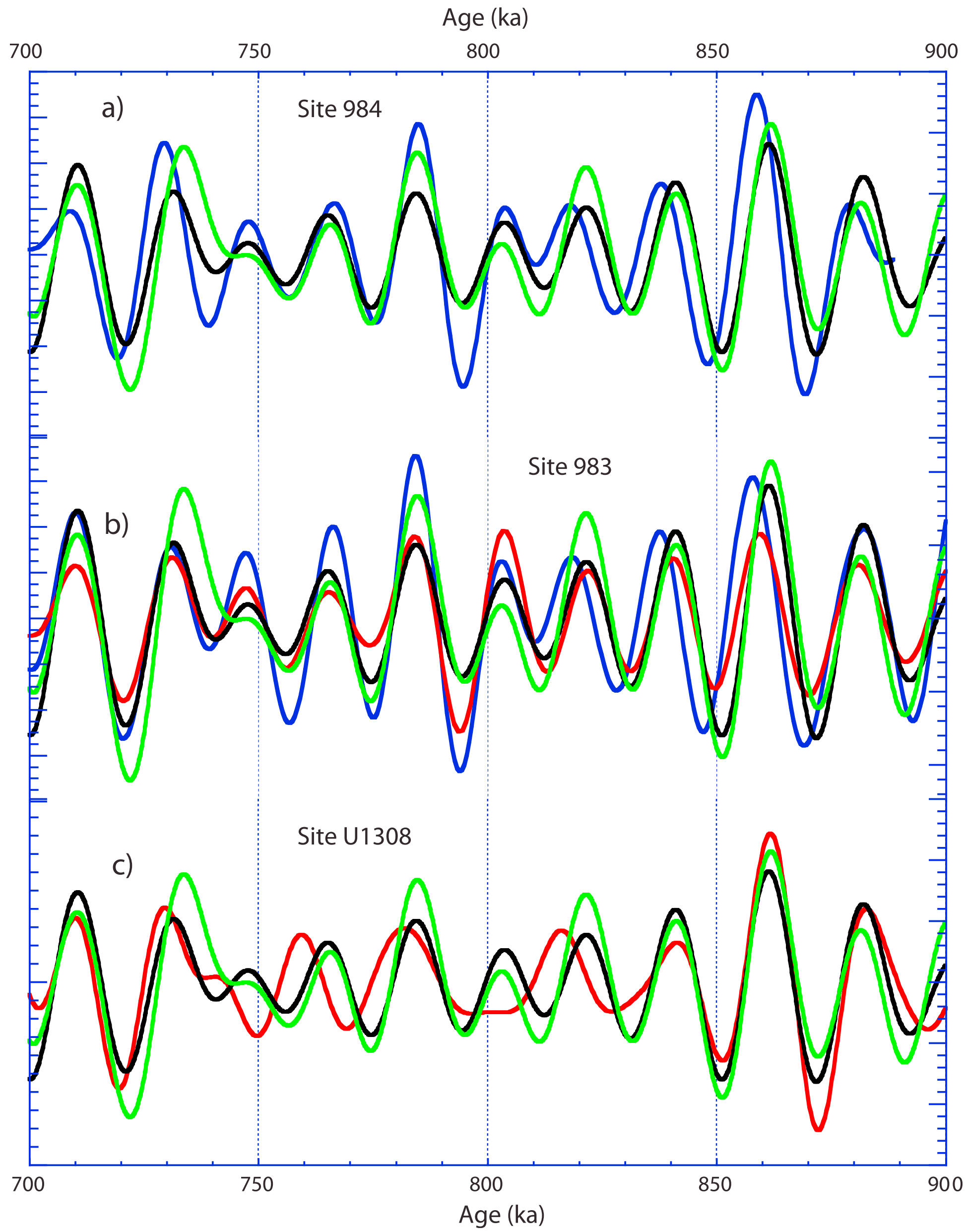

Figure 7. Output of Gaussian band-pass filters centered on a period of 20 kyr applied to planktic (blue) and benthic (red) oxygen isotope records, compared with the output from the same filter applied to the ice volume models constructed from midsummer insolation (black) and integrated summer insolation (light green). There are insufficient benthic data at Site 984 and no planktic data at Site U1308.

with global ice volume as recorded by δ^{18}O (LR04) and Antarctic temperatures as recorded by δD_{ice}. Similar CO_2 oscillations in MIS 3 in the Taylor Dome ice core [*Indermühle et al.*, 2000] coincide with Antarctic Isotope Maximum (AIM) warming events implying that the MIS 19–18 transition has characteristics in common with MIS 3 [*Lüthi et al.*, 2008]. *Pol et al.* [2010] support this conclusion by labeling the δD_{ice} oscillations in the MIS 18–19 transition at Dome C, from younger to older, as AIM A, AIM B and AIM C.

[18] The interhemispheric phasing of millennial-scale climate change during MIS 3 has been inferred by both methane synchronization of Greenland and Antarctic ice cores [*EPICA Community Members*, 2006] and by comparing the timing of planktic and benthic δ^{18}O changes in cores from the Portuguese margin that apparently record both Antarctic and

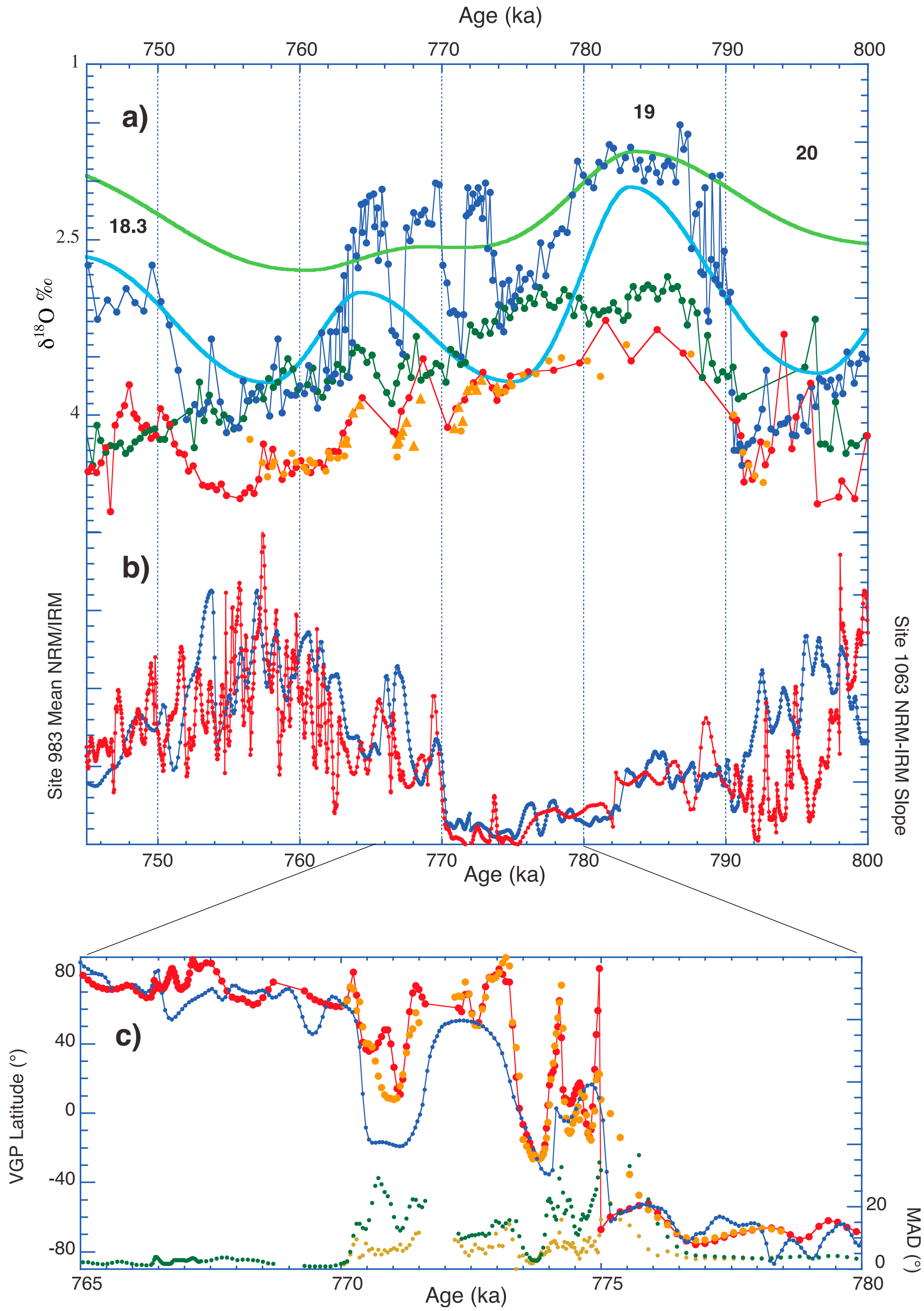

Figure 8. (a) ODP Site 983 planktic (blue) oxygen isotope data [*Channell and Kleiven*, 2000] compared with the IODP Site U1308 benthic (green) oxygen isotope data [*Hodell et al.*, 2008] and the ODP Site 1063 benthic isotope data from *Feretti et al.* [2005] (red with joining line) and Site 1063 benthic data measured at the University of Florida on *Cibicidides wuellerstorfi* (orange circles) and *Oridorsalis umbonatus* (orange triangles) compared with ice volume models based on midsummer (light blue) and integrated summer (light green) insolation forcing. (b) ODP Site 983 (blue) and ODP Site 1063 (red) relative paleointensity proxies. (c) Virtual geomagnetic polar (VGP) latitudes for ODP Site 983 (blue) and ODP Site 1063 (red and orange) where red VGP symbols joined by line and maximum angular deviation (MAD) values (green) represent component magnetizations determined for a fixed 20–80 mT peak field demagnetization range. Orange VGP symbols and MAD values (ocher) represent component magnetizations determined individually (variable peak AF field range) at 1 cm intervals.

Table 1. Age and Duration of the M-B Polarity Transition

Site	Onset Age (ka)	End Age (ka)	Duration (kyr)	Reversal Age (ka)
ODP 980	774.8	771.3	3.5	773.1
ODP 983	775.0	770.4	4.6	772.7
ODP 984	776.5	770.3	6.2	773.4
ODP 1063	775.0	770.4	4.6	772.7
IODP U1308	775.0	772.0	2.9	773.5
Mean reversal age	775.3	770.9	4.4	773.1
SD -1σ (kyr)	0.7	0.7	1.3	0.4
Dome C[a] (EDC2)	773.6	769.8	3.8	771.7
Dome C[a] (EDC3)	768.2	764.7	3.5	766.4

[a]Estimates based on age of ^{10}Be peak [*Raisbeck et al.*, 2006; *Dreyfus et al.*, 2008].

Greenland signals [*Shackleton et al.*, 2000, 2004]. For reasons not well understood [*Skinner et al.*, 2003], the benthic δ^{18}O signal on Portuguese Margin, and elsewhere in the North Atlantic [*Hodell et al.*, 2010], resembles Antarctic temperature variations whereas planktic δ^{18}O records from the same locations mimic stadial-interstadial oscillations in Greenland. By comparing the timing of planktic and benthic δ^{18}O changes, *Shackleton et al.* [2000, 2004] confirmed the phasing deduced by methane synchronization of Greenland and Antarctic ice cores [*Blunier et al.*, 1998; *Blunier and Brook*, 2001; *EPICA Community Members*, 2006]. The Antarctic warm events occur during the longest, coldest stadials in Greenland, and are followed by abrupt warming in Greenland as Antarctica begins to cool. This pattern has been referred to as the "bipolar seesaw" [*Broecker*, 1998] and is explained by changes in heat transport related to thermohaline circulation referred to as Atlantic Meridional Overturning Circulation (AMOC).

[19] The M-B boundary at ODP Site 983 lies within the oldest of the three planktic δ^{18}O minima (Figure 3), at an age that would coincide with the oldest of the δD_{ice} oscillations, on the EDC3 or EDC2 age model, at Dome C (Figure 9). Due to the shielding effect of the geomagnetic field on cosmic ray flux, geomagnetic field intensity can be estimated from cosmogenic isotope flux in ice cores [see *Muscheler et al.*, 2005], and the position of the M-B boundary in the Dome C ice core can be estimated from the flux of ^{10}Be [*Raisbeck et al.*, 2006; *Dreyfus et al.*, 2008]. The median flux ^{10}Be at Dome C shows two broad peaks, separated by about 20 kyr at ~770 and ~790 ka, that appear to correlate with two prominent lows in the paleointensity (RPI) records, particularly in the Site U1308 RPI record (Figure 9). The two lows in paleointensity are less well defined at ODP Sites 980/983/984, although the initial dip in paleointensity at all four sites occurs coincidentally at ~792 ka (Figures 3–5). If we associate the maximum in ^{10}Be flux with the M-B boundary at Dome C, the apparent age of the M-B boundary age in the marine cores is more consistent with the EDC2 age model than the EDC3 age model that yield M-B boundary ages of 772 and 766 ka, respectively (Table 1).

[20] At Site 983, the planktic δ^{18}O minima are phase shifted relative to weakly manifest δ^{18}O oscillations in the benthic record (Figure 10). The decreases in benthic δ^{18}O occur on the MIS 19–18 transition appear to occur at times of maximum planktic δ^{18}O (i.e., cold events). This is similar to MIS 3 when the Antarctic warm events coincide with the Greenland stadials [*EPICA Community Members*, 2006]. Oscillations of similar age are observed in the Site U1308 benthic record (Figure 6) and the Site 1063 benthic record (Figure 8), although the age models are insufficiently precise to resolve synchronicity or phase shifts. Following *Shackleton et al.* [2000, 2004], the benthic δ^{18}O signal from the particular locations in the North Atlantic tracks Antarctic temperature variations. Assuming a similar relationship for Site 983, we synchronize the δD_{ice} at Dome C to the benthic δ^{18}O at Site 983 (Figure 10). The adjustment of the δD_{ice} record from the EDC2/EDC3 age models (Figure 9) results in a close synchronization of increase and decrease in ^{10}Be flux with the onset and end of the directional transition (as indicated by VGP latitude) at the M-B boundary (Figure 10), providing tacit support for the synchronization of the benthic δ^{18}O at Site 983 and the δD_{ice} at Dome C, and hence for the "bipolar seesaw."

5. The ^{40}Ar/^{39}Ar Ages

[21] Due to the sporadic nature of volcanic eruption and the brief (few thousand years) duration of polarity reversal, the capture of magnetization directions recording polarity transitions is highly fortuitous. Arguably, the best constrained ^{40}Ar/^{39}Ar age for the M-B boundary is from the Haleakala caldera on Maui [*Coe et al.*, 2004]. Here, 24 flows over about 36 m of section record transitional magnetization directions characterized by large-scale R-N-R swings in VGP latitude. Six of these flows yielded ^{40}Ar/^{39}Ar ages of 773.0 ± 3.0 ka to 785.1 ± 8.0 ka (not in stratigraphic order) that gave an inverse variance weighted mean of 775.6 ± 1.9 ka [*Coe et al.*, 2004; *Singer et al.*, 2005], relative to $FCs_{28.02}$. The paleomagnetic record at Haleakala (Maui) is complicated by a hiatus in the volcanic

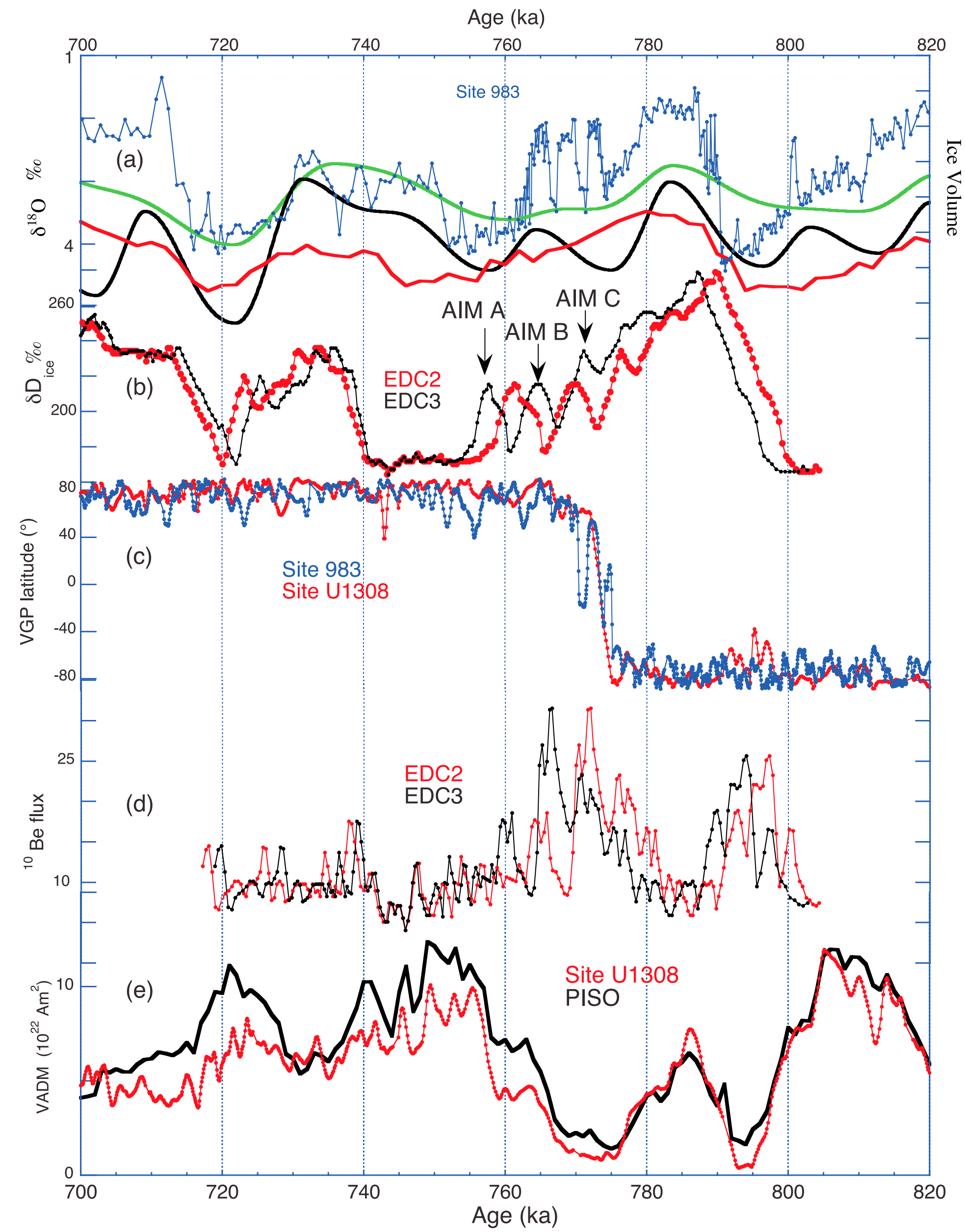

Figure 9. (a) ODP Site 983 planktic oxygen isotope record (blue) placed on the published age model [*Channell and Kleiven*, 2000] compared with the LR04 benthic isotope stack (red) [*Lisiecki and Raymo*, 2005] and with ice volume models based on peak summer (black) and integrated summer (light green) insolation forcing. (b) Dome C δD_{ice} on the EDC2 age model (red) and on the EDC3 age model (black) [*Jouzel et al.*, 2007], with AIM events labeled after *Pol et al.* [2010]. (c) Virtual geomagnetic polar (VGP) latitudes for Site 983 (blue) and Site U1308 (red) denoting the M-B boundary. (d) Median ^{10}Be flux [*Raisbeck et al.*, 2006] placed on the EDC2 age model (red) and EDC3 age model (black). (e) Relative paleointensity proxy for IODP Site U1308 (red) [*Channell et al.*, 2008] correlated to the PISO paleointensity stack [*Channell et al.*, 2009] calibrated to virtual axial dipole moment (VADM).

activity of more than 220 ka. The 24 transitional flows that record the M-B reversal lie directly atop a sequence of 16 flows, also transitionally magnetized, that span about 30 m of section where six $^{40}Ar/^{39}Ar$ determinations give a mean age of 900.3 ± 4.7 ka. These ~900 ka excursional magnetization directions are associated with the Kamikatsura excursion [*Coe et al.*, 2004]. This excursion has not been convincingly recorded in sediments and derives its name from transitional magnetizations in the Kamikatsura Tuff of SW Japan [*Maenaka*, 1983; *Takatsugi and Hyodo*, 1995], and has been

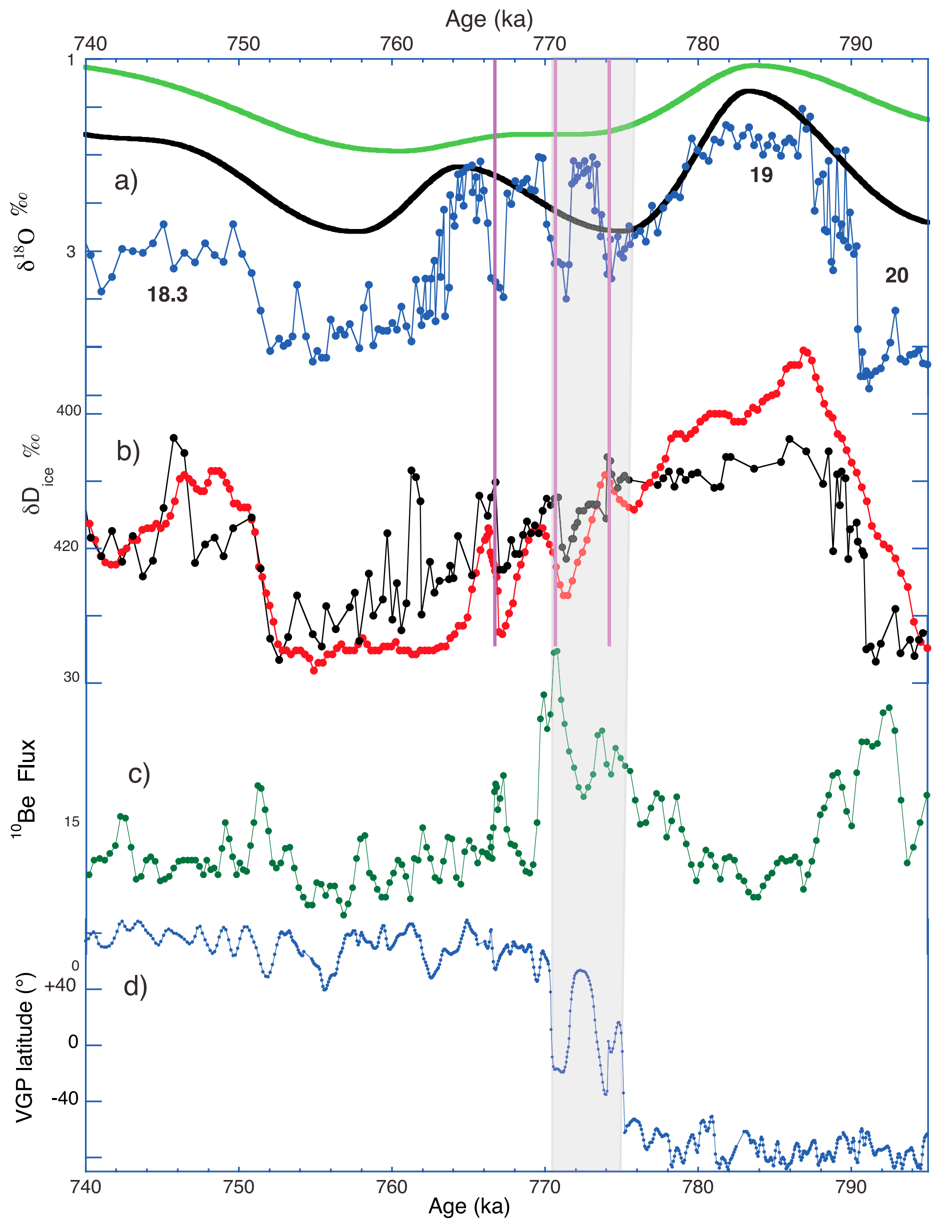

Figure 10. (a) ODP Site 983 planktic oxygen isotope record (blue) placed on the published age model [*Channell and Kleiven*, 2000] compared with ice volume models based on midsummer (black) and integrated summer (light green) insolation forcing. (b) Dome C δD_{ice} (red) from *Jouzel et al.* [2007] shifted in age to correlate with the ODP Site 983 benthic oxygen isotope record (black). Purple vertical lines emphasize the correlation of Site 983 benthic $\delta^{18}O$ (and δD_{ice}) minima to Site 983 plantkic $\delta^{18}O$ maxima (analogous to observations in MIS 3 in the North Atlantic, see text). (c) The median ^{10}Be flux [*Raisbeck et al.*, 2006] placed on the resulting age model for Dome C brings the peak in ^{10}Be flux at 771 ka in coincidence with (d) the change in VGP latitude denoting the Matuyama-Brunhes (M-B) boundary at Site 983. Light gray shading indicates the M-B boundary polarity transition interval at ODP Site 983 and its implied correlation to the Dome C ice core record adjusted in age to synchronize Site 983 benthic $\delta^{18}O$ and δD_{ice}.

identified in a single transitionally magnetized lava flow on Tahiti that is $^{40}Ar/^{39}Ar$ dated relative to $FCs_{28.02}$ at 904 ± 11 ka [*Singer et al.*, 1999].

[22] The 775.6 ka M-B boundary age from Maui becomes 781 ± 2 ka if calculated relative to $FCs_{28.201}$ [*Kuiper et al.*, 2008] and 783.5 ± 2 ka relative to $FCs_{28.305}$ [*Renne et al.*, 2010] (Figure 11). *Kuiper et al.* [2008, Table S3] recalculated 16 published $^{40}Ar/^{39}Ar$ ages applicable to the M-B boundary thereby shifting M-B boundary ages from the 772–800 ka range to the 780–813 ka range. It is appro-

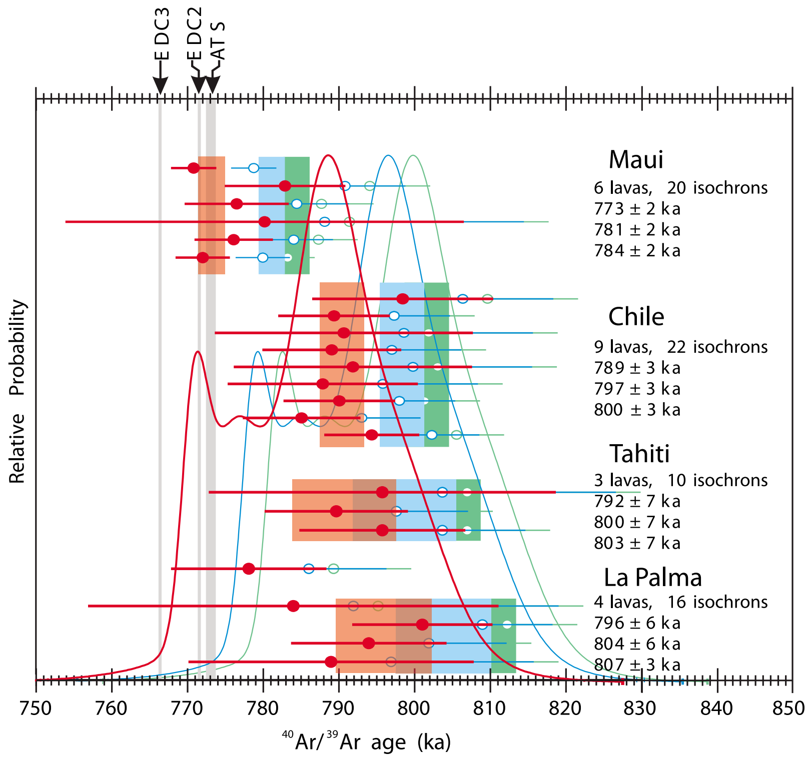

Figure 11. The $^{40}Ar/^{39}Ar$ ages from transitionally magnetized lavas on four volcanoes computed using the $FCs_{28.305}$ calibration (green), $FCs_{28.201}$ calibration (blue), and "optimal" $FCs_{27.93}$ estimate (red). Astrochronological age and uncertainty and EDC2 and EDC3 ages for the Matuyama-Brunhes (M-B) boundary (gray vertical bars) are from Table 1. All uncertainties shown at the two sigma level of precision. Note that for the Maui lavas at the M-B boundary, propagating the full uncertainty of the $FCs_{28.201}$ or the $FCs_{28.305}$ calibrations (including errors in the standard age and ^{40}K decay constant) would result in an uncertainty of ±4 ka, which would double the width of the mean age boxes in blue and green; yet this remains insufficient to bring the $^{40}Ar/^{39}Ar$ ages into overlap with the astrochronological estimate.

priate, when comparing $^{40}Ar/^{39}Ar$ ages to independent astrochronologies, to expand uncertainty estimates to include, in addition to analytical error, intrinsic uncertainties associated with the age of the FCs standard and ^{40}K decay constant. Accordingly, the recalculated Maui M-B age and accompanying uncertainty using $FCs_{28.201}$ [*Kuiper et al.*, 2008] becomes 781 ± 4 ka. Note that the values given by *Kuiper et al.* [2008, Table S3] do not include the full uncertainties. The supposed M-B boundary ages from Chile, Tahiti and La Palma (summarized by *Singer et al.* [2005]) yield average ages of 791.7, 794.8, and 798.4 ka, respectively, relative to $FCs_{28.02}$. Recalculation of these ages to $FCs_{28.201}$ yields ages of 797, 800 and 804 ka, and to $FCs_{28.305}$ yields ages of 800, 803 and 807 ka (Table 2 and Figure 11). Even before recalculation, the M-B boundary age estimates from Chile, Tahiti and La Palma are over 15 kyr older than the estimate from Maui, leading *Singer et al.* [2005] to link the age estimates from Chile, Tahiti and La Palma with transitional magnetization directions associated with a paleointensity low that precedes the M-B boundary, as seen at Site U1308 and Site 980 (Figures 5 and 6) and in the ^{10}Be flux at Dome C (Figure 9). This prereversal paleointensity low has not (as yet) been associated with transitional magnetization directions in sedimentary records.

[23] For reversals and excursions between the M-B boundary and 1.2 Ma, the $FCs_{28.201}$ calibrations yield a consistent discrepancy of 1%–2% (8–21 kyr), reaching over 2% (12–24 kyr) for $FCs_{28.305}$, relative to ages derived from astronomically calibrated marine sediments (Table 2 and Figure 12).

6. Astrochronologies

[24] Astrochronological ages are determined by matching cycles in sedimentary sequences to astronomic solutions for orbital cycles, or to calculations of solar insolation for a particular latitude and time

Table 2. Age Estimates for Reversals and Excursions[a]

	Event and Location								
	M-B, Maui	PreM-B, Chile	PreM-B, Tahiti	PreM-B, La Palma	S. Rosa	Top Jar	Base Jar	Puna	Cobb
Reference[b]	1	1	1	1	2	3	3	3	4
Ar-Ar age in reference (ka)	775.6	791.7	794.8	798.4	936	1001	1069	1122	1193
$FCs_{28.305}$	784	800	803	807	946	1011	1080	1133	1205
$FCs_{28.201}$	781	797	800	804	942	1008	1076	1129	1201
$FCs_{27.93}$	773	789	792	796	933	998	1066	1118	1189
Astro (ka)	773	794	794	794	932	987	1068	1115	1190
EDC2	772	797	797	797					
EDC3	766	794	794	794					

[a]Ages are in ka. M-B, Matuyama-Brunhes boundary; PreM-B, precursor to Matuyama-Brunhes boundary; S. Rosa, Santa Rosa excursion; Top Jar, top of Jaramillo; Base Jar, base of Jaramillo; Puna, Punaruu Excursion; Cobb, Cobb Mountain Subchron; $FCs_{28.305}$, age calculated using 28.305 Ma for the FCs standard [*Renne et al.*, 2010]; $FCs_{28.201}$, age calculated using 28.201 Ma for the FCs standard [*Kuiper et al.*, 2008]; $FCs_{27.93}$, age calculated relative to 27.93 Ma for the FCs standard, chosen to optimally fit astrochronological estimates; Astro, astrochronological age estimates from this paper (M-B and PreM-B) and from *Channell et al.* [2002]; EDC2 and EDC3, EPICA Dome C [*Jouzel et al.*, 2007] age estimates based on peaks in ^{10}Be using the EDC2 and EDC3 age models [*Raisbeck et al.*, 2006; *Dreyfus et al.*, 2008].

[b]References are numbered as follows: 1, *Singer et al.* [2005]; 2, *Singer and Brown* [2002]; 3, *Singer et al.* [1999, 2004]; 4, *Nomade et al.* [2005].

of year. Bedding rhythms, physical property data and geochemical parameters, almost any parameter that appears cyclic in sedimentary sequences, have been matched to astronomic solutions to construct astrochronologies. For eccentricity, the orbital solution is considered to be precise at least over the last 40 Myr, however, the solution for precession and obliquity is less accurate due to uncertainties related to tidal dissipation in the Earth-Moon system. These uncertainties can be gauged by computing the difference between the solution for present-day values of tidal dissipation and half the present-day value

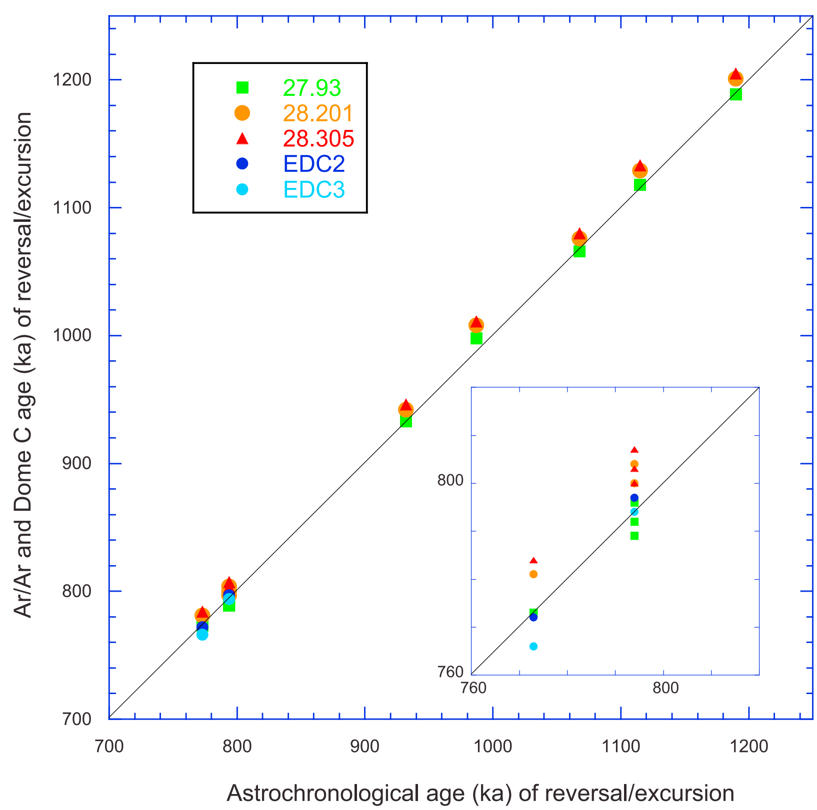

Figure 12. Astronomical estimates and ice core estimates (using EDC 2 and EDC 3 age models) for the ages of geomagnetic reversals and excursions in the 700–1250 ka interval compared with $^{40}Ar/^{39}Ar$ ages calculated relative to $FCs_{27.93}$ (the optimal FCs for consistency with astrochronology), $FCs_{28.201}$, and $FCs_{28.305}$. Data from Table 2.

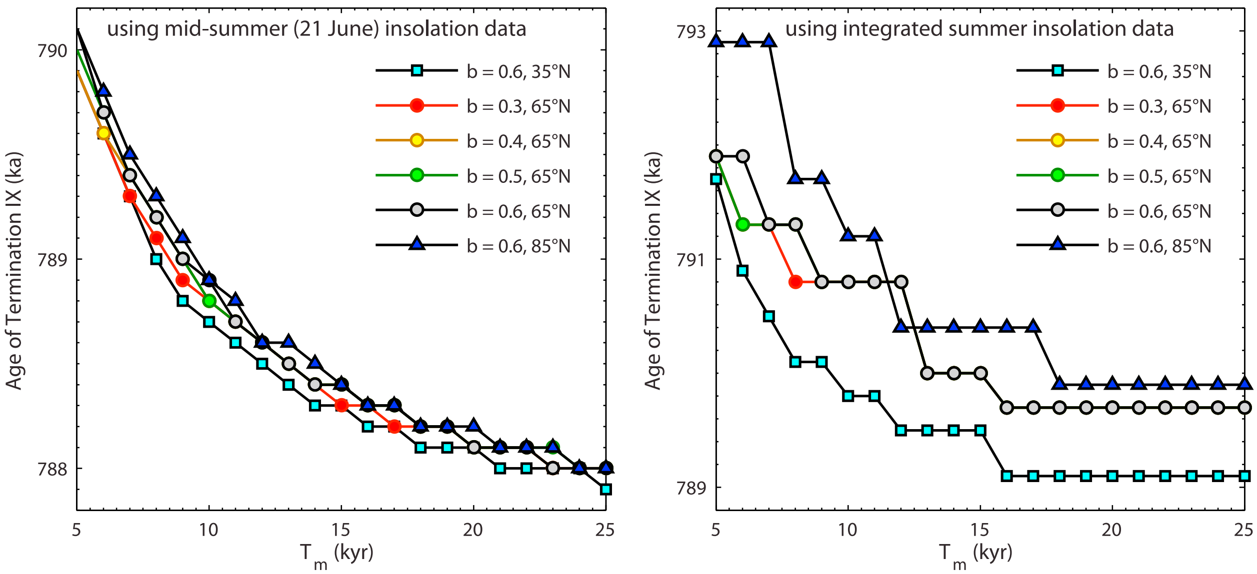

Figure 13. Age of Termination IX (MIS 19/20 boundary) in ice volume models as a function of b (nonlinearity), T_m (mean time constant), and (left) latitude of midsummer insolation and (right) latitude of integrated summer insolation. For integrated summer insolation, an insolation threshold of 275 W/m^2 was used for latitudes other than 35°N, for which 425 W/m^2 was used.

of tidal dissipation, and these differences increase to ~1 cycle for both precession and obliquity at ~15 Ma [*Lourens et al.*, 2004]. For the last few million years, uncertainties in astronomical solutions that use modern values of dynamical ellipticity and tidal dissipation, are probably insignificant, however, another uncertainty comes to the fore for young sequences, namely, the time lag between orbital forcing and response, that may exceed several kyr, and is therefore particularly important for young (Quaternary) ages.

[25] Benthic oxygen isotope records, that are the basis for age models described here, are generally considered to represent a measure of global ice volume, and for this reason, can be used as a global stratigraphic tool, although benthic δ^{18}O record is influenced by changes in benthic temperature and water chemistry [e.g., *Skinner et al.*, 2003; *Sosdian and Rosenthal*, 2009]. Following *Imbrie and Imbrie* [1980], the lag between insolation forcing and response for ice volume is traditionally accommodated by construction of an ice volume model of the form:

$$\frac{dy}{dt} = \frac{1 \pm b}{T_m}(x - y)$$

where the ice volume (y) depends on the insolation forcing (x), a mean time constant (T_m) and a nonlinearity function (b) subtracted during ice growth and added during ice decay. The calculation of insolation requires selection of latitude and time of year, and, according to classic Milankovitch theory, midsummer (21 June) at 65°N is generally selected. *Huybers* [2006] has argued that integrated summer insolation (at 65°N) is a more appropriate forcing function as it incorporates the duration of the summer season. The benthic isotope stack of *Lisiecki and Raymo* [2005], referred to as LR04, was calibrated using an ice volume model constructed from midsummer insolation at 65°N using the orbital solution of *Laskar et al.* [1993] with b and T_m values of 0.6 and 15 kyr, respectively, for the last 1.5 Myr. In LR04, the time constant of 15 kyr was selected to maximize agreement with independent age estimates for the last 135 kyr. For the 5.3–3.0 Ma interval of LR04, values of b and T_m of 0.3 and 5 kyr, respectively, were used with linear increases to values of 0.6 and 15 kyr during the 3.0–1.5 Ma interval.

[26] Termination IX (the MIS 19–20 boundary) is the prominent marker in δ^{18}O records just prior to the M-B boundary. In Figure 13, we test the sensitivity of the age of Termination IX in the ice volume models to changes in b, T_m and the choice of latitude for insolation calculation. Two types of insolation data are used for the test: midsummer insolation calculated using the *Laskar et al.* [2004] orbital solutions, and the integrated summer insolation estimated using the *Huybers* [2006] approach. For the integrated summer insolation, a threshold of

275 W/m^2 is used for the calculation at 65°N and 85°N, and a threshold of 425 W/m^2 is used for the calculation at 35°N. For each ice volume model, the age of Termination IX is determined as the age when the rate of ice volume decrease reaches a maximum within the 810–785 ka interval. Ice volume models calculated using integrated summer insolation yield Termination IX ages about 1–2 kyr older than those estimated using the midsummer insolation data (Figure 13). The value of nonlinearity (b) in the 0.3–0.6 range does not make a difference of more than 0.5 kyr in the age of Termination IX. The most important variable in the ice volume model is the choice of T_m where values ranging from 5 to 15 kyr change the age of the Termination by about 2 kyr (Figure 13). Note little (<0.5 kyr) change in the age of the Termination as T_m increases beyond 15 kyr. For ice volume models calculated using midsummer insolation, low (<0.5 kyr) dependence of Termination age on latitude is observed. Choice of latitude changes the age of Termination IX by about 1–2 kyr if integrated summer insolation is used.

7. Conclusions

[27] The five North Atlantic marine sites discussed here carry the highest-resolution coupled isotope-paleomagnetic records across the M-B boundary. These records have higher resolution (higher sedimentation rates) than records used in earlier analyses of the M-B boundary [e.g., *Tauxe et al.*, 1996; *Leonhardt and Fabian*, 2007; *Suganuma et al.*, 2010]. The recent records, when placed on their independent age models, yield closely consistent estimates for the age of the M-B boundary with a mean age of 773.1 ka, and standard deviation of 0.4 kyr (Table 1). This M-B boundary age is close to the age of the ^{10}Be peak in EPICA Dome C ice core when placed on the EDC2 age model (772 ka), whereas the EDC3 age model yields an even younger age (766 ka). The M-B boundary coincides with the oldest of three millennial-scale fluctuations in planktic and benthic δ^{18}O in the North Atlantic (Figure 3), and with similar oscillations in δD_{ice} at Dome C (Figure 9). At Site 983, the planktic and benthic δ^{18}O oscillations appear out of phase and may be interpreted, following similar observations on Portuguese Margin in MIS 3 [*Shackleton et al.*, 2000, 2004], as out-of-phase Greenland and Antarctic temperature signals manifest in planktic and benthic δ^{18}O, respectively. If Site 983 benthic δ^{18}O is synchronized with δD_{ice} oscillations at Dome C by shifting the δD_{ice} record, consistent with the Portuguese Margin MIS 3 analog, the ice core ^{10}Be flux peak coincides with the marine M-B boundary, thereby supporting the revised age for the M-B boundary.

[28] In three Pacific cores with mean sedimentation rates in the 0.66–1.19 cm/kyr range, the M-B boundary from paleomagnetic measurements is offset down-core by ~15 cm from sedimentary ^{10}Be flux maxima associated with M-B boundary paleointensity minima [*Suganuma et al.*, 2010]. From isotopic tracers, the bioturbated surface layer in pelagic sediments has thickness around 10 cm, varying in the 3–30 cm range, and is largely independent of sedimentation rate [*Boudreau*, 1994, 1998]. The efficiency of mixing in the bioturbated layer [see *Guinasso and Schink*, 1975] is often sufficiently high that remanence acquisition (lock-in) must occur below this layer [see *Channell and Guyodo*, 2004]. Although a 15 cm lock-in depth corresponds to ~15 kyr remanence delay in the Pacific cores studied by *Suganuma et al.* [2010], a similar lock-in depth in the sediments studied here would correspond to a delay in remanence acquisition of ~1 kyr, assuming bioturbation depth and hence lock-in depth are independent of sedimentation rate.

[29] The M-B reversal occurs at the young end of MIS19, at the onset of the transition to MIS 18. Termination IX in LR04 lies at ~788–789 ka because *Lisiecki and Raymo* [2005] calibrated their δ^{18}O stack using an ice volume model forced by midsummer insolation at 65°N with time constant (T_m) equal to 15 kyr, and nonlinearity (b) of 0.6 (Figure 13). For midsummer insolation forcing, values of T_m of 5 kyr would increase the age of the Termination to ~790 ka but the flexibility in age of the Termination is less than 2 kyr for reasonable values of T_m and b (Figure 13). For integrated summer insolation forcing, for $T_m = 15$, the age of Termination IX (at 790 ka) is older by ~2 kyr than for the midsummer insolation calculation using the same variables. In summary, flexibility in ice volume models can account for variations in the age of Termination IX of ~3 kyr.

[30] The observed discrepancy between astrochronological and ^{40}Ar/^{39}Ar age estimates for the M-B boundary and late Matuyama reversals and excursions (Table 2 and Figure 12), when the $FCs_{28.201}$ or the $FCs_{28.305}$ standard age is used, cannot be accounted for by changing variables associated with the ice volume models that provide the astrochronological calibration of benthic δ^{18}O records. The age of the FCs standard that best fits the astrochronological ages is 27.93 Ma, within the

error range of the widely adopted value of 28.02 ± 0.16 Ma [*Renne et al.*, 1998].

[31] The *Kuiper et al.* [2008] $FCs_{28.201}$ calibration of this standard is based on $^{40}Ar/^{39}Ar$ dating of sanidine phenocrysts extracted from tephra layers in the Messinian Melilla Basin (Morocco). The $^{40}Ar/^{39}Ar$ ages were correlated, using six biostratigraphic events, to astrochronologies (based on sapropels and bedding rhythms) in the Sorbas Basin of Spain [*Sierro et al.*, 2001; *van Assen et al.*, 2006]. Sedimentary cycles in the Melilla sections [*Kuiper et al.*, 2008, p. 500] "lack the expression of characteristic details….common in Mediterranean sapropel sequences." The absence of an interpretable cyclostratigraphy in the Melilla sequences from which the $^{40}Ar/^{39}Ar$ ages were derived means that the astrochronological calibration of the Melilla tephras relies heavily on the biostratigraphic correlations between the Melilla and Sorbas basins [*Sierro et al.*, 2001; *van Assen et al.*, 2006]. Note that no usable magnetic stratigraphy was resolved in the Mellila sections [*van Assen et al.*, 2006], and hence the correlation of $^{40}Ar/^{39}Ar$ ages to the magnetic stratigraphy (C3Ar-C3r) in the Sorbas Basin [*Sierro et al.*, 2001] also relies on the correlation of these six biostratigraphic events.

[32] Part of the attraction of the new $FCs_{28.201}$ age, and even more so the $FCs_{28.305}$ calibration, is that it [*Kuiper et al.*, 2008, p. 502] "eliminates the documented offset of the conventionally calibrated $^{40}Ar/^{39}Ar$ and U/Pb dating systems in many volcanic rocks" which has become a problem in geochronology as the analytical precision has improved. However, there are exceptions in the observation of offsets, for example, the normally magnetized Bishop Tuff in California lies just above the M-B boundary in sediment sections across the western USA and laser fusion of sanidine from this unit gives a $^{40}Ar/^{39}Ar$ age of 774 ± 3 ka for the $FCs_{28.02}$ [*Sarna-Wojcicki et al.*, 2000]. Sedimentation rate estimates from the various sections led *Sarna-Wojcicki et al.* [2000] to conclude that the M-B reversal occurred 15 kyr before the eruption of the Bishop Tuff, at 789 ka. If the 774 ka age of the Bishop Tuff is recalculated to 779 ka using $FCs_{28.201}$, the age of the M-B boundary becomes 794 ka, although *Kuiper et al.* [2008] incorrectly report (their Table S3) an age of 791 ka. An age of 794 ka for the M-B boundary would imply that it predates Termination IX, clearly unacceptable. Isotope dilution thermal ionization mass spectrometry of zircons in the Bishop Tuff [*Crowley et al.*, 2007] yields a $^{206}Pb/^{238}U$ age that is indistinguishable from the $^{40}Ar/^{39}Ar$ age of *Sarna-Wojcicki et al.* [2000] using $FCs_{28.02}$. Whereas the $^{206}Pb/^{238}U$ age of the Bishop Tuff requires a large correction for Th/U fractionation, and is thus not without controversy, *Crowley et al.* [2007] were able to use a Th/U ratio of 2.81 measured in quartz-hosted melt inclusions as a reasonable constraint. An exceptionally high melt Th/U ratio of 6.0 would be required to shift the $^{206}Pb/^{238}U$ age to 779 ka, consistent with the sanidine age of *Sarna-Wojcicki et al.* [2000] using $FCs_{28.201}$, and an even more extreme melt Th/U ratio would be required to push the $^{206}Pb/^{238}U$ age to a value consistent with $FCs_{28.305}$. *Kuiper et al.* [2008] noted that their new Fish Canyon standard age pushes $^{40}Ar/^{39}Ar$ ages for the M-B boundary older than astrochronological estimates, and suggested that the M-B boundary (and presumably other reversal/excursion transitions) are diachronous between the marine sediments and the terrestrial lava sequences from which the $^{40}Ar/^{39}Ar$ ages were derived. Based on the systematic age discrepancy in astrochronological and $^{40}Ar/^{39}Ar$ ages using $FCs_{28.201}$ and $FCs_{28.305}$ (Table 2 and Figure 12), there appears to be a fundamental problem with either the $^{40}Ar/^{39}Ar$ and/or the U-Pb dating systems at this level of resolution.

[33] $^{40}Ar/^{39}Ar$ ages using $FCs_{28.02}$ are clearly more compatible with Quaternary astrochronological age estimates than ages using $FCs_{28.201}$ or $FCs_{28.305}$. In spite of its more controversial $^{206}Pb/^{238}U$ age, the Bishop Tuff $^{40}Ar/^{39}Ar$ age most consistent with the M-B boundary astrochronological age is compatible with $FCs_{28.02}$, but not with either $FCs_{28.201}$ or $FCs_{28.305}$. The problem with $FCs_{28.201}$ may stem from the astronomical age model for the Melilla Basin used by *Kuiper et al.* [2008], possibly through facies-related diachroneity of the biostratigraphic events that link the Sorbas Basin (Spain), where the astrochronologies originate, to the Melilla Basin (Morocco), where the $^{40}Ar/^{39}Ar$ ages originate.

[34] Does the problem lie in the dating of the lava flows correlated to the marine astrochronology? The large numbers of $^{40}Ar/^{39}Ar$ incremental heating experiments on groundmass separated from the transitionally magnetized lavas from Maui [*Coe et al.*, 2004] and lavas recording the reversals at the top and base of the Jaramillo subchron and the Punaruu excursion [*Singer et al.*, 1999] reveal no evidence that argon loss may have lowered the ages. Moreover, the $^{40}Ar/^{39}Ar$ ages for the Santa Rosa excursion and Cobb Mountain Subchron (Table 2) are based on laser fusion analyses of sanidine, a mineral widely regarded as resistant to argon loss. We find it difficult to imagine a process whereby the ages of both lava groundmass and sanidine crystals in this large set of lava flows

could be reduced systematically such that they match each of the astrochronologic estimates.

[35] Our findings illustrate that the standardization of the $^{40}Ar/^{39}Ar$ method remains incompletely resolved. Although a FCs age of 27.93 Ma is consistent with the Quaternary astrochronological ages documented here, and is close to the age of 28.02 Ma advocated by *Renne et al.* [1998], *Smith et al.* [2010] find that $FCs_{28.201}$ [from *Kuiper et al.*, 2008] provides consistency between $^{40}Ar/^{39}Ar$ and U-Pb ages for ash beds in the Eocene Green River Formation, indicating that Cenozoic discrepancies between $^{40}Ar/^{39}Ar$ and U-Pb ages are apparently not resolved by choice of any one FCs age, but may be attributed to other issues such as inheritance in U-Pb ages and decay constant uncertainty.

Acknowledgments

[36] We thank Paul Renne, Joel Baker, Matt Heizler, and an anonymous reviewer for journal reviews and Kyle Min and David Sawyer for comments on an early version of the manuscript. Patricia Feretti provided stable isotope data from the M-B boundary interval at ODP Site 1063. Research was supported by NSF through grants OCE-0850413, OCE-1014506, and EAR-0959108.

References

Baksi, A. K., V. Hsu, M. O. McWilliams, and E. Farrar (1992), $^{40}Ar/^{39}Ar$ dating of the Brunhes Matuyama geomagnetic field reversal, *Science*, *256*, 356–357, doi:10.1126/science.256.5055.356.

Bassinot, F. C., L. D. Labeyrie, E. Vincent, X. Quidelleur, N. J. Shackleton, and Y. Lancelot (1994), The astronomical theory of climate and the age of the Brunhes-Matuyama magnetic reversal, *Earth Planet. Sci. Lett.*, *126*, 91–108, doi:10.1016/0012-821X(94)90244-5.

Berger, A., and M. F. Loutre (1988), New insolation values for the climate of the last 10 million years, *Sci. Rep., 1988/13*, Inst. d'Astron. et de Geophys. George Lemaitre, Univ. Catholique de Louvain-la-Neuve, Louvain-la-Neuve, Belgium.

Blunier, T., and E. J. Brook (2001), Timing of millennial scale climate change in Antarctica and Greenland during the last glacial period, *Science*, *291*, 109–112, doi:10.1126/science.291.5501.109.

Blunier, T., et al. (1998), Asynchrony of Antarctic and Greenland climate change during the last glacial period, *Nature*, *394*, 739–743, doi:10.1038/29447.

Boudreau, B. P. (1994), Is burial velocity a master parameter for bioturbation?, *Geochim. Cosmochim. Acta*, *58*, 1243–1249, doi:10.1016/0016-7037(94)90378-6.

Boudreau, B. P. (1998), Mean mixing depth of sediments: The wherefore and the why, *Limnol. Oceanogr.*, *43*, 524–526, doi:10.4319/lo.1998.43.3.0524.

Broecker, W. S. (1998), Paleocean circulation during the last deglaciation: A bipolar seesaw?, *Paleoceanography*, *13*, 119–121, doi:10.1029/97PA03707.

Brown, L. L., B. S. Singer, J. P. C. Pickens, and B. R. Jicha (2004), Paleomagnetic directions and $^{40}Ar/^{39}Ar$ ages from the Tatara-San Pedro volcanic complex, Chilean Andes: Lava record of a Matuyama-Brunhes precursor?, *J. Geophys. Res.*, *109*, B12101, doi:10.1029/2004JB003007.

Channell, J. E. T., and Y. Guyodo (2004), The Matuyama Chronozone at ODP Site 982 (Rockall Bank): Evidence for decimeter-scale magnetization lock-in depths, in *Timescales of the Geomagnetic Field*, *Geophys. Monogr. Ser.*, vol. 145, edited by J. E. T. Channell et al., pp. 205–219, AGU, Washington, D. C.

Channell, J. E. T., and H. F. Kleiven (2000), Geomagnetic palaeointensities and astrochronological ages for the Matuyama-Brunhes boundary and the boundaries of the Jaramillo Subchron: Palaeomagnetic and oxygen isotope records from ODP Site 983, *Philos. Trans. R. Soc. London, Ser. A*, *358*, 1027–1047, doi:10.1098/rsta.2000.0572.

Channell, J. E. T., and B. Lehman (1997), The last two geomagnetic polarity reversals recorded in high-deposition-rate sediment drifts, *Nature*, *389*, 712–715, doi:10.1038/39570.

Channell, J. E. T., and M. E. Raymo (2003), Paleomagnetic record at ODP Site 980 (Feni Drift, Rockall) for the past 1.2 Myrs, *Geochem. Geophys. Geosyst.*, *4*(4), 1033, doi:10.1029/2002GC000440.

Channell, J. E. T., A. Mazaud, P. Sullivan, S. Turner, and M. E. Raymo (2002), Geomagnetic excursions and paleointensities in the Matuyama Chron at Ocean Drilling Program Sites 983 and 984 (Iceland Basin), *J. Geophys. Res.*, *107*(B6), 2114, doi:10.1029/2001JB000491.

Channell, J. E. T., J. H. Curtis, and B. P. Flower (2004), The Matuyama-Brunhes boundary interval (500–900 ka) in North Atlantic drift sediments, *Geophys. J. Int.*, *158*, 489–505, doi:10.1111/j.1365-246X.2004.02329.x.

Channell, J. E. T., D. A. Hodell, C. Xuan, A. Mazaud, and J. S. Stoner (2008), Age calibrated relative paleointensity for the last 1.5 Myr at IODP Site U1308 (North Atlantic), *Earth Planet. Sci. Lett.*, *274*, 59–71, doi:10.1016/j.epsl.2008.07.005.

Channell, J. E. T., C. Xuan, and D. A. Hodell (2009), Stacking paleointensity and oxygen isotope data for the last 1.5 Myr (PISO-1500), *Earth Planet. Sci. Lett.*, *283*, 14–23, doi:10.1016/j.epsl.2009.03.012.

Clement, B. (2004), Dependence of the duration of geomagnetic polarity reversal on site latitude, *Nature*, *428*, 637–640, doi:10.1038/nature02459.

Coe, R. S., B. S. Singer, M. S. Pringle, and X. Zhao (2004), Matuyama-Brunhes reversal and Kamikatsura event on Maui: Paleomagnetic directions, $^{40}Ar/^{39}Ar$ ages and implications, *Earth Planet. Sci. Lett.*, *222*, 667–684, doi:10.1016/j.epsl.2004.03.003.

Crowley, J. L., B. Schoene, and S. A. Bowring (2007), U-Pb dating of zircon in the Bishop Tuff at the millennial scale, *Geology*, *35*, 1123–1126, doi:10.1130/G24017A.1.

Dreyfus, G. B., et al. (2007), Anomalous flow below 2700 m in the EPICA Dome C ice core detected using $\delta^{18}O$ of atmospheric oxygen measurements, *Clim. Past Discuss.*, *3*, 63–93, doi:10.5194/cpd-3-63-2007.

Dreyfus, G. B., G. M. Raisbeck, F. Perrenin, J. Jouzel, Y. Goyodo, S. Nomade, and A. Mazaud (2008), An ice core perspective on the age of the Matuyama-Brunhes boundary, *Earth Planet. Sci. Lett.*, *274*, 151–156, doi:10.1016/j.epsl.2008.07.008.

EPICA Community Members (2004), Eight glacial cycles from an Antarctic ice core, *Nature*, *429*, 623–628, doi:10.1038/nature02599.

EPICA Community Members (2006), One-to-one coupling of glacial climate variability in Greenland and Antarctica, *Nature*, *444*, 796–798.

Feretti, P., N. J. Shackleton, D. Rio, and M. A. Hall (2005), Early Middle Pleistocene deep circulation in the western subtropical Atlantic: Southern Hemisphere modulation of the North Atlantic Ocean, in *Early Middle Pleistocene Transitions: The Land-Ocean Evidence*, edited by M. J. Head and P. L. Gibbard, *Geol. Soc. Spec. Publ.*, *247*, 131–145.

Guinasso, N. L., and D. R. Schink (1975), Quantitative estimates of biological mixing rates in abyssal sediments, *J. Geophys. Res.*, *80*, 3032–3043, doi:10.1029/JC080i021p03032.

Hodell, D. A., J. E. T. Channell, J. H. Curtis, O. Romero, and U. Röhl (2008), Onset of "Hudson Strait" Heinrich events in the eastern North Atlantic at the end of the middle Pleistocene transition (~640 ka)?, *Paleoceanography*, *23*, PA4218, doi:10.1029/2008PA001591.

Hodell, D. A., H. F. Evans, J. E. T. Channell, and J. H. Curtis (2010), Phase relationships of North Atlantic ice rafted debris and surface-deep climate proxies during the last glacial period, *Quat. Sci. Rev.*, in press.

Huybers, P. (2006), Early Pleistocene glacial cycles and the integrated summer insolation forcing, *Science*, *313*, 508–511, doi:10.1126/science.1125249.

Imbrie, J., and J. Z. Imbrie (1980), Modeling the climate response to orbital variations, *Science*, *207*, 943–953, doi:10.1126/science.207.4434.943.

Imbrie, J., J. Hays, D. Martinson, A. McIntyre, A. Mix, J. Morley, N. Pisias, W. Prell, and N. J. Shackleton (1984), The orbital theory of Pleistocene climate: Support from a revised chronology of the marine $\delta^{18}O$ record, in *Milankovitsch and Climate, Part 1*, edited by A. Berger et al., pp. 269–305, D. Reidel, Hingham, Mass.

Indermühle, A., E. Monnin, B. Stauffer, T. F. Stocker, and M. Wahlen (2000), Atmospheric CO_2 concentration from 60 to 20 kyr BP from the Taylor Dome ice core, Antarctica, *Geophys. Res. Lett.*, *27*, 735–738, doi:10.1029/1999GL010960.

Johnson, R. G. (1982), Brunhes-Matuyama magnetic reversal dated at 790,000 yr B.P. by marine-astronomical correlations, *J. Quat. Res.*, *17*, 135–147, doi:10.1016/0033-5894(82)90055-2.

Jouzel, J., et al. (2007), Orbital and millennial Antarctic climate variability over the past 800,000 years, *Science*, *317*, 793–796, doi:10.1126/science.1141038.

Kirschvink, J. L. (1980), The least squares lines and plane analysis of paleomagnetic data, *Geophys. J. R. Astron. Soc.*, *62*, 699–718.

Kuiper, K. F., A. Deino, F. J. Hilgen, W. Krijgsman, P. F. Renne, and J. R. Wijbrans (2008), Synchronizing rock clocks of Earth history, *Science*, *320*, 500–504, doi:10.1126/science.1154339.

Laskar, J., F. Joutel, and F. Boudin (1993), Orbital, precessional and insolation quantities for the Earth from −20 Myr to +10 Myr, *Astron. Astrophys.*, *270*, 522–533.

Laskar, J., P. Robutel, F. Joutel, M. Gastineau, A. Correia, and B. Levrard (2004), A long term numerical solution for the insolation quantities of the Earth, *Astron. Astrophys.*, *428*, 261–285, doi:10.1051/0004-6361:20041335.

Leonhardt, R., and K. Fabian (2007), Paleomagnetic reconstruction of the global geomagnetic field evolution during the Matuyama/Brunhes transition: Iterative Bayesian inversion and independent verification, *Earth Planet. Sci. Lett.*, *253*, 172–195, doi:10.1016/j.epsl.2006.10.025.

Linsley, B. K., and M. T. von Breymann (1991), Stable isotopic and geochemical record in the Sulu Sea during the last 7500 k.y.: Assessment of surface water variability and paleoproductivity changes, *Proc. Ocean Drill. Program Sci. Results*, *124*, 379–396.

Lisiecki, L. E., and M. E. Raymo (2005), A Pliocene-Pleistocene stack of 57 globally distributed benthic $\delta^{18}O$ records, *Paleoceanography*, *20*, PA1003, doi:10.1029/2004PA001071.

Lourens, L. J., F. J. Hilgen, J. Laskar, N. J. Shackleton, and D. Wilson (2004), The Neogene period, in *A Geologic Time Scale 2004*, edited by F. M. Gradstein, J. G. Ogg, and A. G. Smith, pp. 409–440, Cambridge Univ. Press, Cambridge, U. K.

Lüthi, D., et al. (2008), High resolution carbon dioxide concentration record 650,000–800,000 years before present, *Nature*, *453*, 379–382, doi:10.1038/nature06949.

Maenaka, K. (1983), Magnetostratigraphic study of the Osaka Group, with special reference to the existence of pre and post-Jaramillo episodes in the Late Matuyama Polarity Epoch, *Mem. Hanazono Univ.*, *14*, pp. 1–65, Hanazono Univ., Kyoto, Japan.

Mankinen, E. A., and G. B. Dalrymple (1979), Revised geomagnetic polarity time scale for the interval 0–5 m.y. B.P., *J. Geophys. Res.*, *84*, 615–626, doi:10.1029/JB084iB02p00615.

Muscheler, R., J. Beer, P. W. Kublik, and H. A. Synal (2005), Geomagnetic field intensity during the last 60,000 years based on ^{10}Be and ^{36}Cl from the Summit ice cores and ^{14}C, *Quat. Sci. Rev.*, *24*, 1849–1860, doi:10.1016/j.quascirev.2005.01.012.

Nomade, S., P. R. Renne, N. Vogel, A. L. Deino, W. D. Sharp, T. A. Becker, A. R. Jaouni, and R. Mundil (2005), Alder Creek sanidine (ACs-2): A Quaternary $^{40}Ar/^{39}Ar$ dating standard tied to the Cobb Mountain geomagnetic event, *Chem. Geol.*, *218*, 315–338, doi:10.1016/j.chemgeo.2005.01.005.

Oda, H., S. Hidetoshi, and V. Hsu (2000), Paleomagnetic records of the Brunhes/Matuyama polarity transition from ODP Leg 124(Celebes and Sulu seas), *Geophys. J. Int.*, *142*, 319–338, doi:10.1046/j.1365-246x.2000.00130.x.

Parrenin, F., et al. (2007), Ice flow modeling at EPICA Dome C and Dome Fuji, East Antarctica, *Clim. Past Discuss.*, *3*, 19–61, doi:10.5194/cpd-3-19-2007.

Pol, K., et al. (2010), New MIS 19 EPICA Dome C high resolution deuterium data: Hints for a problematic preservation of climate variability at sub-millennial scale in the "oldest ice," *Earth Planet. Sci. Lett.*, doi:10.1016/j.epsl.2010.07.030, in press.

Raisbeck, G. M., F. Yiou, O. Cattani, and J. Jouzel (2006), ^{10}Be evidence for the Matuyama-Brunhes geomagnetic reversal in the EPICA Dome C ice core, *Nature*, *444*, 82–84, doi:10.1038/nature05266.

Raymo, M. E., D. W. Oppo, B. P. Flower, D. A. Hodell, J. F. McManus, K. A. Venz, K. F. Kleiven, and K. McIntyre (2004), Stability of North Atlantic water masses in face of pronounced climate variability during the Pleistocene, *Paleoceanography*, *19*, PA2008, doi:10.1029/2003PA000921.

Renne, P. R., C. C. Swisher, A. L. Deino, D. B. Karner, T. L. Owens, and D. J. DePaolo (1998), Intercalibration of standards, absolute ages and uncertainties in $^{40}Ar/^{39}Ar$ dating, *Chem. Geol.*, *145*, 117–152, doi:10.1016/S0009-2541(97)00159-9.

Renne, P. R., R. Mundil, G. Balco, K. Min, and K. R. Ludwig (2010), Joint determination of ^{40}K decay constants and $^{40}Ar^*/^{40}K$ for the Fish Canyon sanidine standard, and improved accuracy for $^{40}Ar/^{39}Ar$ geochronology, *Geochim. Cosmochim. Acta*, *74*, 5349–5367, doi:10.1016/j.gca. 2010.06.017.

Ruddiman, W. F., M. E. Raymo, D. G. Martinson, B. M. Clement, and J. Backman (1989), Pleistocene evolution: Northern Hemisphere ice sheet and North Atlantic Ocean, *Paleoceanography*, *4*, 353–412, doi:10.1029/PA004i004p00353.

Sarna-Wojcicki, A. M., M. Pringle, and J. Wijbrans (2000), New ^{40}Ar/^{39}Ar age of the Bishop Tuff from multiple sites and sediment rate calibration for the Matuyama-Brunhes boundary, *J. Geophys. Res.*, *105*, 21,431–21,443.

Shackleton, N. J., A. Berger, and W. R. Peltier (1990), An alternative astronomical calibration of the lower Pleistocene timescale based on ODP Site 677, *Trans. R. Soc. Edinburgh*, *81*, 251–261.

Shackleton, N. J., M. A. Hall, and E. Vincent (2000), Phase relationships between millennial-scale events 64,000–24,000 years ago, *Paleoceanography 15*, 565–569, doi:10.1029/2000PA000513.

Shackleton, N. J., R. G. Fairbanks, T.-C. Chiu, and F. Parrenin (2004), Absolute calibration of the Greenland time scale: Implications for Antarctic time scales and for Δ^{14}C, *Quat. Sci. Rev.*, *23*, 1513–1522, doi:10.1016/j.quascirev.2004.03.006.

Shipboard Scientific Party (1998), Bermuda Rise and Sohm Abyssal Plain, Sites 1063 and 1064, *Proc. Ocean Drill. Program Initial Rep.*, *172*, 251–308.

Sierro, F. J., F. J. Hilgen, W. Krijsman, and J. A. Flores (2001), The Abad composite (SE Spain): A Messinian reference section for the Mediterranean and the APTS, *Palaeogeogr. Palaeoclimatol. Palaeoecol.*, *168*, 141–169, doi:10.1016/S0031-0182(00)00253-4.

Singer, B., and L. L. Brown (2002), The Santa Rosa event: ^{40}Ar/^{39}Ar and paleomagnetic results from the Valles rhyolite near Jaramillo Creek, Jemez Mountains, New Mexico, *Earth Planet. Sci. Lett.*, *197*, 51–64, doi:10.1016/S0012-821X(01)00598-2.

Singer, B. S., and M. S. Pringle (1996), Age and duration of the Matuyama-Brunhes geomagnetic polarity transition from ^{40}Ar/^{39}Ar incremental heating analyses of lavas, *Earth Planet. Sci. Lett.*, *139*, 47–61, doi:10.1016/0012-821X(96)00003-9.

Singer, B. S., K. A. Hoffman, A. Chauvin, R. S. Coe, and M. S. Pringle (1999), Dating transitionally magnetized lavas of the late Matuyama Chron: Toward a new ^{40}Ar/^{39}Ar timescale of reversals and events, *J. Geophys. Res.*, *104*, 679–693, doi:10.1029/1998JB900016.

Singer, B. S., M. R. Relle, K. A. Hoffman, A. Battle, H. Guillou, C. Laj, and J. C. Carracedo (2002), Ar/Ar ages from transitionally magnetized lavas on La Palma, Canary Islands, and the geomagnetic instability timescale, *J. Geophys. Res.*, *107*(B11), 2307, doi:10.1029/2001JB001613.

Singer, B. S., L. L. Brown, J. O. Rabassa, and H. Guillou (2004), ^{40}Ar/^{39}Ar chronology of late Pliocene and Early Pleistocene geomagnetic and glacial events in southern Argentina, in *Timescales of the Paleomagnetic Field*, *Geophys. Monogr. Ser.*, vol. 145, edited by J. E. T. Channell et al., pp. 175–190, AGU, Washington, D. C.

Singer, B. S., K. A. Hoffman, R. S. Coe, L. L. Brown, B. R. Jicha, M. S. Pringle, and A. Chauvin (2005), Structural and temporal requirements for geomagnetic field reversal deduced from lava flows, *Nature*, *434*, 633–636, doi:10.1038/nature03431.

Skinner, L. C., N. J. Shackleton, and H. Elderfield (2003), Millennial-scale variability of deep-water temperature and $\delta^{18}O_{dw}$ indicating deep-water source variations in the Northeast Atlantic, 0–34 cal. ka BP, *Geochem. Geophys. Geosyst.*, *4*(12), 1098, doi:10.1029/2003GC000585.

Smith, M. E., K. R. Chamberlain, B. S. Singer, and A. E. Carroll (2010), Eocene clocks agree: Coeval ^{39}Ar/^{40}Ar, U-Pb and astronomical ages from the Green River Formation, *Geology*, *38*, 527–530, doi:10.1130/G30630.1.

Sosdian, S., and Y. Rosenthal (2009), Deep-sea temperature and ice volume changes across the Pliocene-Pleistocene climate transitions, *Science*, *325*, 306–310, doi:10.1126/science.1169938.

Steiger, R. H., and E. Jaeger (1977), Subcommission on geochronology: Convention on the use of decay constants in geo- and cosmochronology, *Earth Planet. Sci. Lett.*, *36*, 359–362, doi:10.1016/0012-821X(77)90060-7.

Suganuma, Y., Y. Yokoyama, T. Yamazaki, K. Kawamura, C.-S. Horng, and H. Matsuzaki (2010), ^{10}Be evidence for delayed acquisition of remanent magnetization in marine sediments: Implications for a new age for the Matuyama-Brunhes boundary, *Earth Planet. Sci. Lett.*, *296*, 443–450, doi:10.1016/j.epsl.2010.05.031.

Takatsugi, K. O., and M. Hyodo (1995), A geomagnetic excursion during the late Matuyama Chron, the Osaka group, southwest Japan, *Earth Planet. Sci. Lett.*, *136*, 511–524, doi:10.1016/0012-821X(95)00175-C.

Tauxe, L., T. Herbert, N. J. Shackleton, and Y. S. Kok (1996), Astronomical calibration of the Matuyama-Brunhes boundary: Consequences for magnetic remanence acquisition in marine carbonates and the Asian loess sequences, *Earth Planet. Sci. Lett.*, *140*, 133–146, doi:10.1016/0012-821X(96)00030-1.

van Assen, E., K. F. Kuiper, N. Barboun, W. Krijgsman, and F. J. Sierro (2006), Messinian astrochronology of the Melilla Basin: Stepwise restriction of the Mediterranean-Atlantic connection through Morocco, *Palaeogeogr. Palaeoclimatol. Palaeoecol.*, *238*, 15–31, doi:10.1016/j.palaeo.2006.03.014.